NASA/CR-1998-207637
ICASE Report No. 98-17

The Wavelet Element Method Part II: Realization and Additional Features in 2D and 3D

Claudio Canuto and Anita Tabacco
Politecnico di Torino, Italy

Karsten Urban
Institut fur Geometrie und Praktische Mathematik, Germany

Institute for Computer Applications in Science and Engineering
NASA Langley Research Center
Hampton, VA

Operated by Universities Space Research Association

National Aeronautics and
Space Administration

Langley Research Center
Hampton, Virginia 23681-2199

Prepared for Langley Research Center
under Contract NAS1-97046

April 1998

Available from the following:

NASA Center for AeroSpace Information (CASI)
7121 Standard Drive
Hanover, MD 21076-1320
(301) 621-0390

National Technical Information Service (NTIS)
5285 Port Royal Road
Springfield, VA 22161-2171
(703) 487-4650

THE WAVELET ELEMENT METHOD
PART II: REALIZATION AND ADDITIONAL FEATURES IN 2D AND 3D *

CLAUDIO CANUTO†, ANITA TABACCO‡, AND KARSTEN URBAN§

Abstract. The Wavelet Element Method (WEM) provides a construction of multiresolution systems and biorthogonal wavelets on fairly general domains. These are split into subdomains that are mapped to a single reference hypercube. Tensor products of scaling functions and wavelets defined on the unit interval are used on the reference domain. By introducing appropriate matching conditions across the interelement boundaries, a globally continuous biorthogonal wavelet basis on the general domain is obtained. This construction does not uniquely define the basis functions but rather leaves some freedom for fulfilling additional features.

In this paper we detail the general construction principle of the WEM to the 1D, 2D and 3D cases. We address additional features such as symmetry, vanishing moments and minimal support of the wavelet functions in each particular dimension. The construction is illustrated by using biorthogonal spline wavelets on the interval.

Key words. wavelet element method, matching conditions.

Subject classification. Applied and Numerical Mathematics

1. Introduction. The construction of multiresolution systems and wavelets on general domains and manifolds in $\mathbb{R}^n$ is a crucial issue for applying wavelet methods to the numerical solution of operator equations such as partial differential and integral equations. This problem has been recently addressed by many authors [15, 7, 13, 4, 14, 10, 16].

In [4], the *Wavelet Element Method* (WEM) was introduced borrowing ideas from analogous constructions in spectral methods. Tensor products of scaling functions and wavelets on the unit interval are mapped to the subdomains in which the original domain is split. By matching these functions across the interelement boundaries, globally continuous biorthogonal wavelet systems are obtained, which allow the characterization of certain function spaces and their duals. These spaces contain functions which are piecewise regular with respect to a Sobolev or Besov scale in each subdomain, and satisfy suitable matching conditions at the interfaces.

The construction of [4] does not uniquely determine one particular wavelet basis. It rather indicates the algebraic conditions to be satisfied in order to obtain a globally matched basis, leaving the freedom of enforcing additional features for the basis. The purpose of the present paper is to exploit this freedom,

*This research was partially supported by the National Aeronautics and Space Administration under NASA Contract No. NAS1-97046, while the first author was in residence at the Institute for Computer Applications in Science and Engineering (ICASE), NASA Langley Research Center, Hampton, VA 23681-2199. Other support come from the following funds: in Italy, MURST ex-40% *Analisi Numerica, Progetto Strategico CNR Modelli e Metodi per la Matematica e l'Ingegneria, Progetto Coordinato CNR Wavelets, analisi del segnale e simmetrie* and *Progetto Vigoni*; in Germany, DAAD VIGONI–Project *Multilevel-Zerlegungsverfahren für Partielle Differentialgleichungen* and VOLKSWAGEN–Stiftung within the project *Reduzierte Modellierung und Simulation von Vielstoffprozessen mit Multiskalen-Verfahren.*

†Dipartimento di Matematica, Politecnico di Torino, Corso Duca degli Abruzzi 24, 10129 Torino, Italy, and Istituto di Analisi Numerica del C.N.R., 27100 Pavia, Italy, e-mail: `ccanuto@polito.it`.

‡Dipartimento di Matematica, Politecnico di Torino, Corso Duca degli Abruzzi 24, 10129 Torino, Italy, e-mail: `tabacco@polito.it`.

§Institut für Geometrie und Praktische Mathematik, RWTH Aachen, Templergraben 55, 52056 Aachen, Germany, e-mail: `urban@igpm.rwth-aachen.de`.

indicating how to construct wavelet bases that have properties such as, e.g., minimal local support, moment conditions or symmetry.

While [4] deals with the general spatial dimension n, here we detail our construction in the univariate, bivariate and trivariate cases separately, showing additional properties in each particular dimension. Following the guidelines given in this paper, one can concretely build scaling functions and wavelets (as well as the related transforms) on fairly general domains starting from a given multiresolution analysis on the unit interval. As an example, we illustrate the results of our construction when a biorthogonal spline wavelet system on the interval is used. The filter coefficients for this example are given in the Appendix. An application to the numerical solution of 2D elliptic boundary value problems is presented in [5].

The outline of the paper is as follows. In Section 2 we recall the main properties of biorthogonal systems on cubes, which may fulfil homogeneous boundary conditions. Section 3 is devoted to the description of the multiresolution analyses on general domains. The construction of the corresponding wavelets in 1D, 2D and 3D is described in Sections 4, 5 and 6, respectively.

2. Biorthogonal systems on reference domains. In this section, we use tensor products to construct scaling functions and biorthogonal wavelets on hypercubes starting from suitable multiresolution analyses on the unit interval (eventually fulfilling homogeneous boundary conditions).

We will frequently use the following notation: by $A \lesssim B$ we denote the fact that A can be bounded by a multiple constant times B, where the constant is independent of the various parameters A and B may depend on. Furthermore, $A \lesssim B \lesssim A$ (with different constants, of course) will be abbreviated by $A \sim B$.

2.1. General setting on the interval $[0,1]$. There are many examples of biorthogonal wavelets on the interval available in the literature, see [2, 9, 18, 6, 11, 17] for example. In this subsection we collect the main properties of those biorthogonal wavelet systems on the interval constructed in [11, 17]. We first describe the general approach and then the modifications for fulfilling boundary conditions as introduced in [4, 13].

The starting point are two families of *scaling functions*

$$\Xi_j := \{\xi_{j,k} : k \in \Delta_j\},\ \tilde{\Xi}_j := \{\tilde{\xi}_{j,k} : k \in \Delta_j\} \subset L^2(0,1),$$

where Δ_j denotes an appropriate set of indices and $j \geq j_0$ can be understood as the scale parameter (with some j_0 denoting the coarsest scale). For subsequent convenience, these functions will not be labeled by integers as usual, but rather by a set of real indices

$$\Delta_j := \{\tau_{j,1}, \dots, \tau_{j,K_j}\}, \qquad 0 = \tau_{j,1} < \tau_{j,2} < \cdots < \tau_{j,K_j} = 1. \tag{2.1}$$

In other words, each basis function is associated with a *node*, or grid point, in the interval $[0,1]$; the actual position of the internal nodes $\tau_{j,2}, \dots, \tau_{j,K_j-1}$ will be irrelevant in the sequel, except that it is required that $\Delta_j \subset \Delta_{j+1}$ (see (2.3-h)). It will be also convenient to consider Ξ_j as the column vector $(\xi_{j,k})_{k\in\Delta_j}$, and analogously for other sets of functions.

The families Ξ_j, $\tilde{\Xi}_j$ can be constructed to be *dual generator systems* of a *multiresolution analysis* in $L^2(0,1)$

$$S_j := \operatorname{span} \Xi_j, \qquad \tilde{S}_j := \operatorname{span} \tilde{\Xi}_j, \tag{2.2}$$

in the sense that the following conditions in (2.3) are fulfilled:

(2.3-a) *The systems* Ξ_j *and* $\tilde{\Xi}_j$ *are* refinable, *i.e., there exist matrices* $M_j, \tilde{M}_j$, *such that*

$$\Xi_j = M_j\, \Xi_{j+1}, \qquad \tilde{\Xi}_j = \tilde{M}_j\, \tilde{\Xi}_{j+1}.$$

This implies, in particular, that the induced spaces S_j, $\tilde{S}_j$ *are* nested, *i.e.,* $S_j \subset S_{j+1}$, $\tilde{S}_j \subset \tilde{S}_{j+1}$.

(2.3-b) *The functions have local support:* $\operatorname{diam}(\operatorname{supp}\xi_{j,k}) \sim \operatorname{diam}(\operatorname{supp}\tilde{\xi}_{j,k}) \sim 2^{-j}$.

(2.3-c) *The systems are* biorthogonal, *i.e.,* $(\xi_{j,k}, \tilde{\xi}_{j,k'})_{L^2(0,1)} = \delta_{k,k'}$, *for all* $k, k' \in \Delta_j$.

(2.3-d) *The systems* Ξ_j, $\tilde{\Xi}_j$ *are* uniformly stable, *i.e.,*

$$\Big\| \sum_{k\in\Delta_j} c_k\, \xi_{j,k} \Big\|_{L^2(0,1)} \sim \|\mathbf{c}\|_{\ell^2(\Delta_j)} \sim \Big\| \sum_{k\in\Delta_j} c_k\, \tilde{\xi}_{j,k} \Big\|_{L^2(0,1)},$$

where $\mathbf{c} := (c_k)_{k\in\Delta_j}$.

(2.3-e) *The functions are* regular, *i.e.,* $\xi_{j,k} \in H^{\gamma}(0,1)$, $\tilde{\xi}_{j,k} \in H^{\tilde{\gamma}}(0,1)$, *for some* $\gamma, \tilde{\gamma} > 1$, *where* $H^s(0,1)$, $s \geq 0$, *denotes the usual Sobolev space on the interval as defined, e.g., in [1].*

(2.3-f) *The systems are* exact *of order* L, $\tilde{L} \geq 1$, *respectively, i.e., polynomials up to the degree* $L-1$, $\tilde{L}-1$ *are reproduced exactly:* $\mathbb{P}_{L-1}(0,1) \subset S_j$, $\mathbb{P}_{\tilde{L}-1}(0,1) \subset \tilde{S}_j$, *where* $\mathbb{P}_r(0,1)$ *denotes the set of the algebraic polynomials of degree* r *at most, restricted to* $[0,1]$.

(2.3-g) *There exist biorthogonal complement spaces* T_j *and* $\tilde{T}_j$ *such that*

$$S_{j+1} = S_j \oplus T_j, \quad T_j \perp \tilde{S}_j, \qquad \tilde{S}_{j+1} = \tilde{S}_j \oplus \tilde{T}_j, \quad \tilde{T}_j \perp S_j.$$

(2.3-h) *The spaces* T_j *and* $\tilde{T}_j$ *have bases*

$$\Upsilon_j = \{\eta_{j,h} : h \in \nabla_j\}, \qquad \tilde{\Upsilon}_j = \{\tilde{\eta}_{j,h} : h \in \nabla_j\},$$

(with $\nabla_j := \Delta_{j+1} \setminus \Delta_j = \{\nu_{j,1}, \ldots, \nu_{j,M_j}\}$, $0 < \nu_{j,1} < \cdots < \nu_{j,M_j} < 1$*) which are biorthogonal (in the sense of* (2.3-c)*) and uniformly stable (in the sense of* (2.3-d)*). These basis functions are called* biorthogonal wavelets.

(2.3-i) *The systems* Ξ_j *and* Υ_j *are* boundary adapted, *i.e., at each boundary point:*

(i) only one basis function in each system is not vanishing; precisely,

$$\xi_{j,k}(0) \neq 0 \iff k = 0, \qquad \xi_{j,k}(1) \neq 0 \iff k = 1, \tag{2.3-i.1}$$

$$\eta_{j,h}(0) \neq 0 \iff h = \nu_{j,1}, \qquad \eta_{j,h}(1) \neq 0 \iff h = \nu_{j,M_j}; \tag{2.3-i.2}$$

(ii) the nonvanishing scaling and wavelet functions take the same value; precisely, there exist constants c_0 *and* c_1 *independent of* j *such that*

$$\xi_{j,0}(0) = \eta_{j,\nu_{j,1}}(0) = c_0 2^{j/2}, \qquad \xi_{j,1}(1) = \eta_{j,\nu_{j,M_j}}(1) = c_1 2^{j/2}. \tag{2.3-i.3}$$

The same holds for the dual systems $\tilde{\Xi}_j$ *and* $\tilde{\Upsilon}_j$.

(2.3-j) *The system* Ξ_j *is* boundary symmetric, *i.e.,* $\xi_{j,0}(0) = \xi_{j,1}(1) =: \lambda_j$ *and also for* $\tilde{\Xi}_j$. □

In addition, thanks to Jackson and Bernstein-type inequalities, these systems yield norm equivalences for a whole range in the Sobolev scale:

$$\Big\| \sum_{k\in\Delta_{j_0}} c_{j_0,k}\, \xi_{j_0,k} + \sum_{j=j_0}^{\infty} \sum_{h\in\nabla_j} d_{j,h}\eta_{j,h} \Big\|_{X^s}^2 \sim \sum_{k\in\Delta_{j_0}} 2^{2sj_0}|c_{j_0,k}|^2 + \sum_{j=j_0}^{\infty} \sum_{h\in\nabla_j} 2^{2sj}\,|d_{j,h}|^2, \tag{2.4}$$

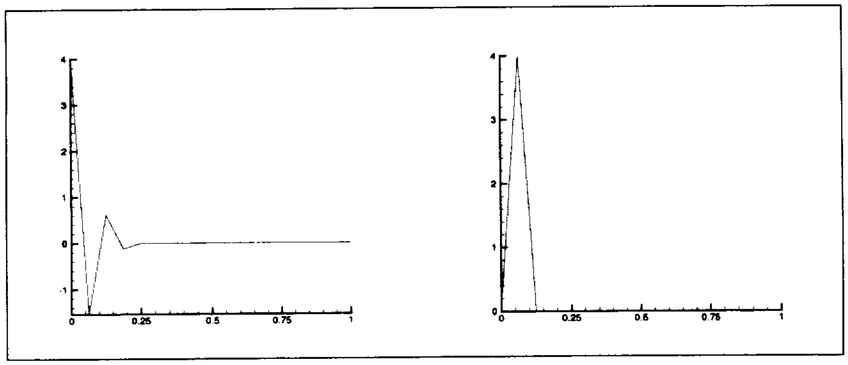

FIG. 2.1. *Primal scaling functions.*

where $s \in \big(-\min(\tilde{L},\tilde{\gamma}), \min(L,\gamma)\big)$ and $X^s = H^s(0,1)$ if $s \geq 0$ or $X^s = (H^{-s}(0,1))'$ if $s < 0$. In particular, for $s = 0$ we have a *Riesz basis* of $L^2(0,1)$.

The following concept will be important in the sequel. The system Ξ_j is said to be *reflection invariant*, if Δ_j is invariant under the mapping $x \mapsto 1-x$ and

$$\xi_{j,k}(1-x) = \xi_{j,1-k}(x), \qquad \text{for all } x \in [0,1] \text{ and } k \in \Delta_j. \tag{2.5}$$

A similar definition can be given for the system Υ_j, as well as for the dual systems. If Ξ_j is reflection invariant, then Υ_j can be built to have the same property. This will be always implicitly assumed.

Example. *Throughout the paper, we shall illustrate our construction of matched scaling functions and wavelets starting from biorthogonal spline wavelets on the real line, as introduced in [8]. The corresponding multiresolutions on the interval are built as in [11, 12] with the choice of parameters $L = 2$ and $\tilde{L} = 4$, using SVD for the biorthogonalization. The particular implementation used to produce the pictures of the present paper is described in [3]. Figures 2.1 and 2.2 show the primal and dual scaling functions which are boundary adapted, whereas Figures 2.3 and 2.4 refer to primal and dual wavelets. These, and all the subsequent Figures of the paper, correspond to the level $j = 4$.* □

2.2. Homogeneous boundary conditions on the interval. Boundary adapted generator and wavelet systems can be easily modified to fulfill homogeneous Dirichlet boundary conditions. To this end, let us first introduce the following sets of the *internal* grid points:

$$\Delta_j^{int} := \Delta_j \setminus \{0,1\}, \qquad \nabla_j^{int} := \nabla_j \setminus \{\nu_{j,1}, \nu_{j,M_j}\}. \tag{2.6}$$

Let us collect in the vector $\beta = (\beta_0, \beta_1) \in \{0,1\}^2$ the information about where homogeneous boundary conditions are enforced, i.e., $\beta_d = 1$ means no boundary condition, whereas $\beta_d = 0$ denotes boundary condition at the point $d \in \{0,1\}$. Correspondingly, let us set

$$\Delta_j^\beta := \begin{cases} \Delta_j^{int}, & \text{if } \beta = (0,0), \\ \Delta_j \setminus \{0\}, & \text{if } \beta = (0,1), \\ \Delta_j \setminus \{1\}, & \text{if } \beta = (1,0), \\ \Delta_j, & \text{if } \beta = (1,1). \end{cases} \tag{2.7}$$

Let the generator systems be defined as

$$\Xi_j^\beta := \{\xi_{j,k} : k \in \Delta_j^\beta\}, \qquad \tilde{\Xi}_j^\beta := \{\tilde{\xi}_{j,k} : k \in \Delta_j^\beta\},$$

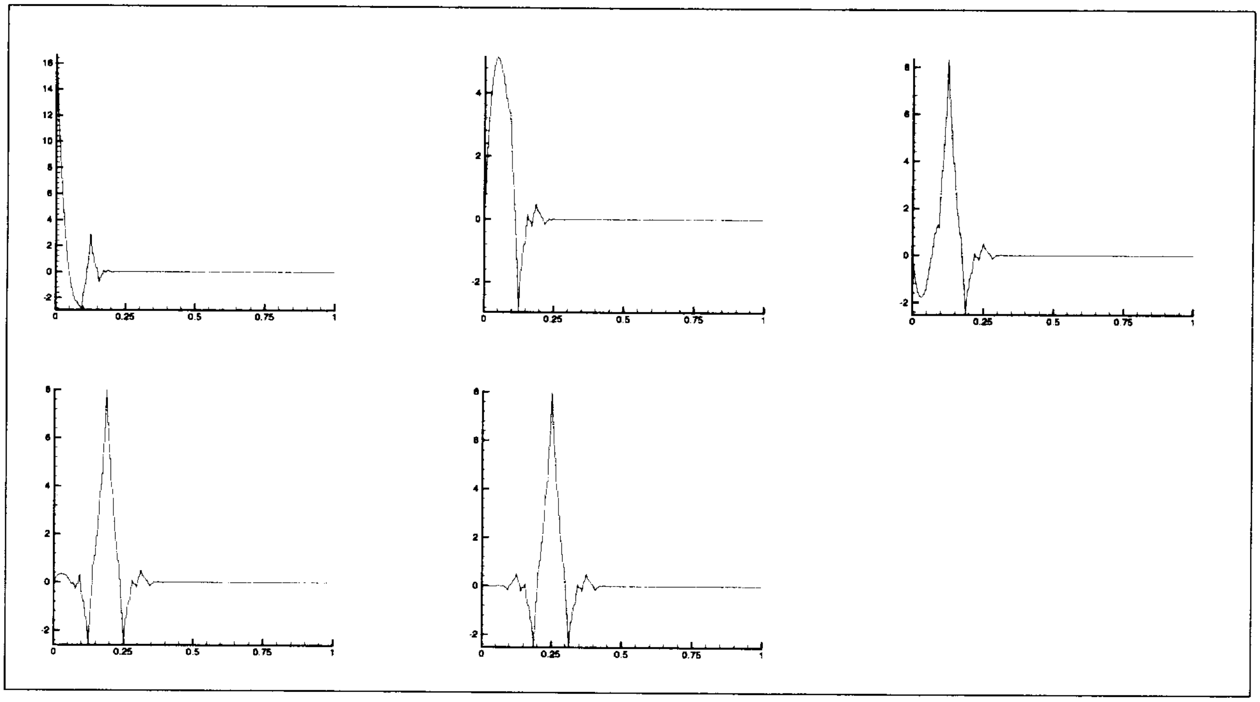

FIG. 2.2. *Dual scaling functions.*

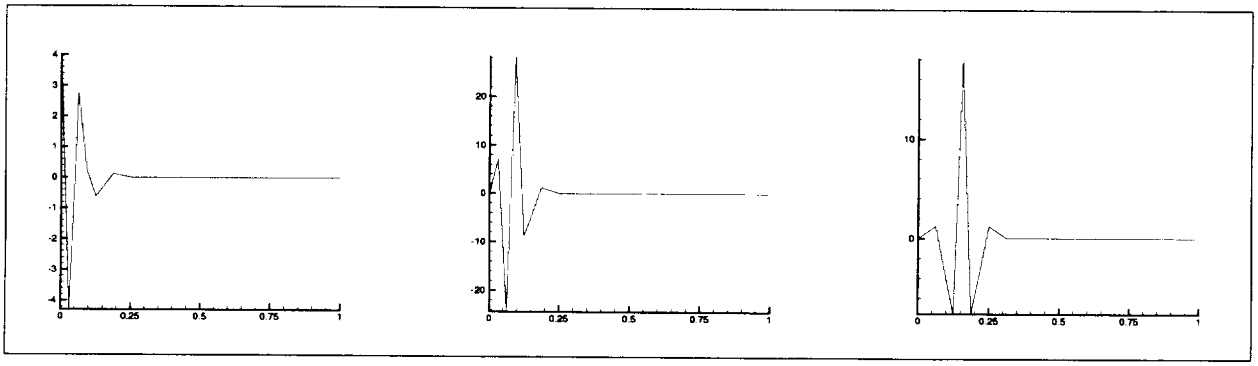

FIG. 2.3. *Primal wavelets.*

and let us define the multiresolution analyses

$$S_j^\beta := \operatorname{span} \Xi_j^\beta, \qquad \tilde{S}_j^\beta := \operatorname{span} \tilde{\Xi}_j^\beta. \tag{2.8}$$

Note that we have simply omitted the scaling functions which do not vanish at those end points of the interval where boundary conditions are enforced.

The associated biorthogonal wavelet systems Υ_j^β, $\tilde{\Upsilon}_j^\beta$ are the same as the previously defined ones, except that we possibly change the first and/or the last wavelet depending on β. More precisely, the wavelets can be chosen to vanish at each boundary point in which the corresponding component of β is zero. If the boundary condition is prescribed at 0, the first wavelets $\eta_{j,\nu_{j,1}}$ and $\tilde{\eta}_{j,\nu_{j,1}}$ are replaced by

$$\eta_{j,\nu_{j,1}}^D := \frac{1}{\sqrt{2}}\,(\eta_{j,\nu_{j,1}} - \xi_{j,0}), \qquad \tilde{\eta}_{j,\nu_{j,1}}^D := \frac{1}{\sqrt{2}}\,(\tilde{\eta}_{j,\nu_{j,1}} - \tilde{\xi}_{j,0}), \tag{2.9}$$

respectively. The wavelets $\eta_{j,\nu_{j,M_j}}^D$ and $\tilde{\eta}_{j,\nu_{j,M_j}}^D$ vanishing at 1 are defined similarly. Observe that the set of grid points ∇_j^β which labels the wavelets does not change, i.e., $\nabla_j^\beta = \nabla_j$ for all choices of β.

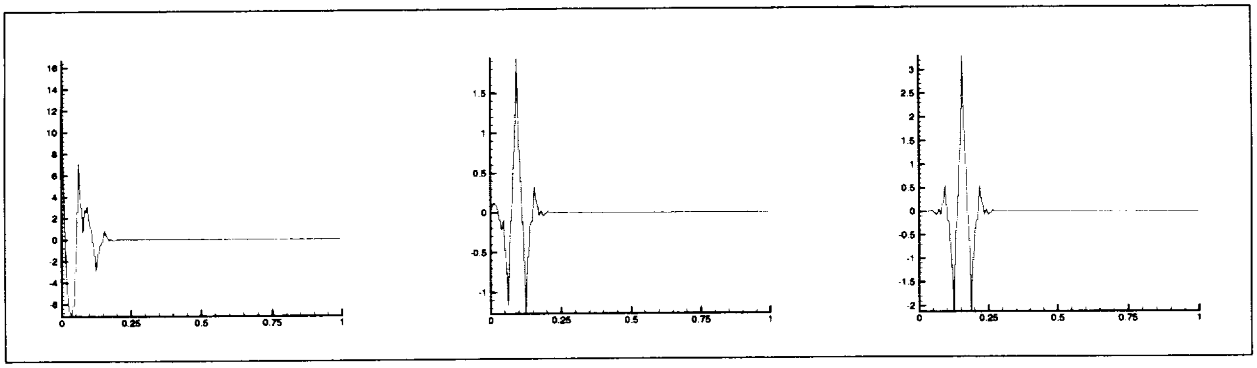

FIG. 2.4. *Dual wavelets.*

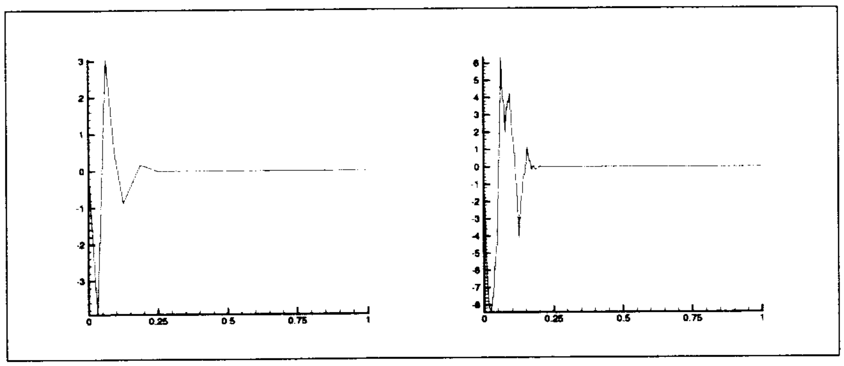

FIG. 2.5. *Primal and dual wavelet corresponding to the first wavelet grid point having homogeneous boundary conditions.*

The new systems Ξ_j^β, Υ_j^β and $\tilde{\Xi}_j^\beta$, $\tilde{\Upsilon}_j^\beta$ fulfill the conditions in (2.3) stated above, provided the index β is appended to all symbols. In addition, if the systems Ξ_j and $\tilde{\Xi}_j$ are reflection invariant, see (2.5), the systems with boundary conditions can be built to be reflection invariant as well, in an obvious sense (i.e., the mapping $x \mapsto 1-x$ induces a mapping of Ξ_j^β into itself if $\beta = (0,0)$ or $\beta = (1,1)$, while it produces an exchange of $\Xi_j^{(0,1)}$ with $\Xi_j^{(1,0)}$ in the other cases).

Example (continued). *Figure 2.5 shows the modified wavelets defined in* (2.9) *for the B–spline multiresolution chosen to illustrate our construction.* □

2.3. Tensor products. Multivariate generators and wavelets can be easily built from univariate ones using tensor products. Hereafter, we describe the construction in the domain $\hat{\Omega} = (0,1)^n$, which will serve as a reference domain later on.

Let the vector $b = (\beta^1, \ldots, \beta^n)$ (where $\beta^l \in \{0,1\}^2$ for $1 \le l \le n$) contain the information on the boundary conditions to be enforced. Let us set, for all $j \ge j_0$,

$$V_j^b(\hat{\Omega}) := S_j^{\beta^1} \otimes \cdots \otimes S_j^{\beta^n},$$

and similarly for $\tilde{V}_j^b(\hat{\Omega})$. These spaces are trivially nested. In order to construct a basis for them, we define for $\hat{x} = (\hat{x}_1, \ldots, \hat{x}_n) \in \hat{\Omega}$ and $\hat{k} = (\hat{k}_1, \ldots, \hat{k}_n) \in \Delta_j^b := \Delta_j^{\beta^1} \times \cdots \times \Delta_j^{\beta^n}$

$$\hat{\varphi}_{j,\hat{k}}(\hat{x}) := (\xi_{j,\hat{k}_1} \otimes \cdots \otimes \xi_{j,\hat{k}_n})(\hat{x}) \;=\; \prod_{l=1}^{n} \xi_{j,\hat{k}_l}(\hat{x}_l);$$

we set

$$\hat{\Phi}_j := \{\hat{\varphi}_{j,\hat{k}} : \hat{k} \in \Delta_j^b\},$$

so that

$$V_j^b(\hat{\Omega}) = \text{span}\,(\hat{\Phi}_j), \qquad \tilde{V}_j^b(\hat{\Omega}) = \text{span}\,(\hat{\tilde{\Phi}}_j).$$

Biorthogonal complement spaces $W_j^b(\hat{\Omega})$, i.e., spaces satisfying

$$V_{j+1}^b(\hat{\Omega}) = V_j^b(\hat{\Omega}) \oplus W_j^b(\hat{\Omega}), \qquad W_j^b(\hat{\Omega}) \perp \tilde{V}_j^b(\hat{\Omega}),$$

are defined as follows. Set $\nabla_j^b := \Delta_{j+1}^b \setminus \Delta_j^b$ and for any $\hat{h} = (\hat{h}_1, \ldots, \hat{h}_n) \in \nabla_j^b$, define the corresponding wavelet

$$\hat{\psi}_{j,\hat{h}}(\hat{x}) := (\hat{\vartheta}_{\hat{h}_1} \otimes \cdots \otimes \hat{\vartheta}_{\hat{h}_n})(\hat{x}) \;=\; \prod_{l=1}^{n} \hat{\vartheta}_{\hat{h}_l}(\hat{x}_l),$$

where

$$\hat{\vartheta}_{\hat{h}_l} := \begin{cases} \xi_{j,\hat{h}_l}, & \text{if } \hat{h}_l \in \Delta_j^{\beta^l}, \\ \eta_{j,\hat{h}_l}, & \text{if } \hat{h}_l \in \nabla_j. \end{cases}$$

Then, set

$$\hat{\Psi}_j := \{\hat{\psi}_{j,\hat{h}} : \hat{h} \in \nabla_j^b\}, \qquad \text{and} \qquad W_j(\hat{\Omega}) := \text{span}\,\hat{\Psi}_j.$$

The definition of $\hat{\tilde{\Psi}}_j$ and $\tilde{W}_j^b(\hat{\Omega})$ is similar. The wavelet systems $\hat{\Psi}_j$ and $\hat{\tilde{\Psi}}_j$ are biorthogonal and form Riesz bases in $L^2(\hat{\Omega})$: the norm equivalences (2.4) extend to the multivariate case as well.

Finally, considering the boundary values, we note that, given any $l \in \{1, \ldots, n\}$ and $d \in \{0, 1\}$, we have

$$(\hat{\varphi}_{j,\hat{k}})_{|\hat{x}_l = d} \equiv 0 \qquad \text{iff} \qquad \hat{k}_l \neq d \;\text{ or }\; (\hat{k}_l = d \text{ and } \beta_d^l = 0)$$

and

$$(\hat{\psi}_{j,\hat{h}})_{|\hat{x}_l = d} \equiv 0 \qquad \text{iff} \qquad \hat{h}_l \neq \nu_d \;\text{ or }\; (\hat{h}_l = \nu_d \text{ and } \beta_d^l = 0),$$

with $\nu_d = \nu_{j,1}$ if $d = 0$, and $\nu_d = \nu_{j,M_j}$ if $d = 1$.

3. Multiresolution on general domains. In this section, we describe the construction of a multiresolution analysis on our domain of interest $\Omega \subset I\!R^n$. As already mentioned, Ω is split into subdomains Ω_i, which are images of the reference element $\hat{\Omega} = (0,1)^n$ under appropriate parametric mappings . The multiresolution analysis on Ω is then obtained by transformations of properly matched systems on $\hat{\Omega}$.

We will first describe our technical assumptions on Ω and the parametric mappings from the reference domain to the subdomains. In Subsection 3.2, we detail the construction of scaling functions and wavelets on a subdomain. The matching for the scaling functions will be described in Subsection 3.3. Most of the wavelets in Ω simply arise by a mapping from the reference element without any matching; these functions will be described in Subsection 3.4. The more complex matching for the wavelets will be detailed in the subsequent sections for the 1D, 2D and 3D cases, separately. Finally, in Subsection 3.5, certain characterization properties of Sobolev spaces are summarized.

3.1. Domain decomposition and parametric mappings. Let us consider our domain of interest $\Omega \subset I\!R^n$, with Lipschitz boundary $\partial\Omega$[1].The boundary $\partial\Omega$ is subdivided in two relatively open parts (with respect to $\partial\Omega$), the Dirichlet part Γ_{Dir} and the Neumann part Γ_{Neu}, in such a way that

$$\overline{\partial\Omega} = \bar{\Gamma}_{\text{Dir}} \cup \bar{\Gamma}_{\text{Neu}}, \qquad \Gamma_{\text{Dir}} \cap \Gamma_{\text{Neu}} = \emptyset.$$

[1]Note that also certain domains that do not have Lipschitz boundary can be treated by this approach. Indeed, we have to assume that Ω can be split into subdomains in such a way, that the assumptions on the parametric mappings are fulfilled.

We assume that there exist N open disjoint subdomains $\Omega_i \subseteq \Omega$ ($i = 1, \dots, N$) such that

$$\bar{\Omega} = \bigcup_{i=1}^{N} \bar{\Omega}_i$$

and such that, for some $r \geq \gamma$ (see (2.3-e)), there exist r-time continuously differentiable mappings $F_i : \bar{\hat{\Omega}} \to \bar{\Omega}_i$ ($i = 1, \dots, N$) satisfying

$$\Omega_i = F_i(\hat{\Omega}), \qquad |JF_i| := \det(JF_i) > 0 \text{ in } \bar{\hat{\Omega}}, \tag{3.1}$$

where JF_i denotes the Jacobian of F_i; in the sequel, it will be useful to set $G_i := F_i^{-1}$.

Let us first set some notation, starting with the reference domain $\hat{\Omega}$. For $0 \leq p \leq n-1$, a *p-face* of $\hat{\Omega}$ is a subset $\hat{\sigma} \subset \partial\hat{\Omega}$ defined by the choice of a set $\mathcal{L}_{\hat{\sigma}}$ of different indices $l_1, \dots, l_{n-p} \in \{1, \dots, n\}$ and a set of integers $d_1, \dots, d_{n-p} \in \{0, 1\}$ in the following way

$$\hat{\sigma} = \{(\hat{x}_1, \dots, \hat{x}_n) \ : \ \hat{x}_{l_1} = d_1, \ \dots, \ \hat{x}_{l_{n-p}} = d_{n-p}, \text{ and } 0 \leq \hat{x}_l \leq 1 \text{ if } l \notin \mathcal{L}_{\hat{\sigma}}\} \tag{3.2}$$

(thus, e.g., in 3D, a 0-face is a vertex, a 1-face is a side and a 2-face is a usual face of the reference cube). The coordinates $\hat{x}_l$ with $l \in \mathcal{L}_{\hat{\sigma}}$ will be termed the *frozen coordinates* of $\hat{\sigma}$, whereas the remaining coordinates will be termed the *free coordinates* of $\hat{\sigma}$.

Next, we set up the technical assumptions for the mappings F_i. To formulate these, we need some notations. Let $\hat{\sigma}$ and $\hat{\sigma}'$ be two p-faces of $\hat{\Omega}$, and let $H : \hat{\sigma} \to \hat{\sigma}'$ be a bijective mapping. We shall say that H is *order-preserving* if it is a composition of elementary permutations $(s,t) \mapsto (t,s)$ of the free coordinates of $\hat{\sigma}$. An order-preserving mapping is a particular case of an affine mapping (see [4], Lemma 4.1).

The image of a p-face of $\hat{\Omega}$ under the mapping F_i will be termed a p-face of Ω_i; if $\Gamma_{i,i'} := \partial\Omega_i \cap \partial\Omega_{i'}$ is nonempty for some $i \neq i'$, then we assume that $\Gamma_{i,i'}$ is a p-face of both Ω_i and $\Omega_{i'}$ for some $0 \leq p \leq n-1$. In addition, setting $\Gamma_{i,i'} = F_i(\hat{\sigma}) = F_{i'}(\hat{\sigma}')$, with two p-faces $\hat{\sigma}$ and $\hat{\sigma}'$ of $\hat{\Omega}$, we require that the bijection $H_{i,i'} := G_{i'} \circ F_i : \hat{\sigma} \to \hat{\sigma}'$ fulfills the following *Hypothesis (3.3):*

a) $H_{i,i'}$ is affine;

b) in addition, if the systems of scaling functions and wavelets on $[0,1]$ are *not* reflection invariant (see (2.5)), then $H_{i,i'}$ is order preserving.

Finally, the decomposition is assumed to be *conformal* in the following sense: the intersection $\bar{\Omega}_i \cap \bar{\Omega}_{i'}$ for $i \neq i'$ is either empty or a p face, $0 \leq p \leq n-1$; moreover, for $i = 1, \dots, N$ we suppose that $\partial\Omega_i \cap \bar{\Gamma}_{\text{Dir}}$ and $\partial\Omega_i \cap \bar{\Gamma}_{\text{Neu}}$ are (possibly empty) unions of p-faces of Ω_i.

To summarize, we need the following assumptions:

(a) The mappings $F_i : \bar{\hat{\Omega}} \to \bar{\Omega}_i$ are r-times continuously differentiable, with $r \geq \gamma$, and satisfy $|JF_i| > 0$ in $\bar{\hat{\Omega}}$;

(b) The mappings F_i fulfill Hypothesis 3.3 above;

(c) The domain decomposition is conformal.

3.2. Multiresolution and wavelets on the subdomains. Let us now introduce multiresolution analyses on each Ω_i, $i = 1, \dots, N$, by "mapping" appropriate multiresolution analyses on $\hat{\Omega}$. To this end, let us define the vector $b(\Omega_i) = (\beta^1, \dots, \beta^n) \in \{0,1\}^{2n}$ as follows

$$\beta_d^l = \begin{cases} 0, & \text{if } F_i(\{\hat{x}_l = d\}) \subset \Gamma_{\text{Dir}}, \\ 1, & \text{otherwise,} \end{cases} \qquad l = 1, \dots, n, \quad d = 0, 1.$$

Moreover, let us introduce the one-to-one transformation $v \mapsto \hat{v} := v \circ F_i$, which maps functions defined in $\bar{\Omega}$ into functions defined in $\bar{\hat{\Omega}}$. Next, for all $j \geq j_0$, let us set

$$V_j(\Omega_i) := \{v \, : \, \hat{v} \in V_j^{b(\Omega_i)}(\hat{\Omega})\}.$$

A basis in this space is obtained as follows. For any $\hat{k} \in \Delta_j^{b(\Omega_i)}$, set $k^{(i)} := F_i(\hat{k})$; then, define the set of grid points

$$\mathcal{K}_j^i := \{k^{(i)} \; : \; \hat{k} \in \Delta_j^{b(\Omega_i)}\}$$

in $\bar{\Omega}_i$. The grid point k, whose image under G_i is $\hat{k}$, is associated with the function in $V_j(\Omega_i)$

$$\varphi_{j,k}^{(i)} := \hat{\varphi}_{j,\hat{k}} \circ G_i,$$

i.e., $\widehat{\varphi_{j,k}^{(i)}} = \hat{\varphi}_{j,\hat{k}}$. The set of all these functions will be denoted by Φ_j^i. This set and the dual set $\tilde{\Phi}_j^i$ form biorthogonal bases of $V_j(\Omega_i)$ and $\tilde{V}_j(\Omega_i)$, respectively, with respect to the inner product in $L^2(\Omega_i)$

$$\langle u, v\rangle_{\Omega_i} := \int_{\Omega_i} u(x)\, v(x)\, |JG_i(x)|\, dx = \int_{\hat{\Omega}} \hat{u}(\hat{x})\, \hat{v}(\hat{x})\, d\hat{x}, \tag{3.4}$$

which, due to the properties of the transformation of the domains, induces an equivalent L^2 type norm

$$\|v\|^2_{L^2(\Omega_i)} \;\sim\; \langle v, v\rangle_{\Omega_i} \;=\; \|\hat{v}\|^2_{L^2(\hat{\Omega})}, \qquad \forall v \in L^2(\Omega_i).$$

Coming to the detail spaces, a complement of $V_j(\Omega_i)$ in $V_{j+1}(\Omega_i)$ can be defined as

$$W_j(\Omega_i) := \{w \, : \, \hat{w} \in W_j^{b(\Omega_i)}(\hat{\Omega})\}.$$

A basis Ψ_j^i in this space is associated with the grid

$$\mathcal{H}_j^i := \mathcal{K}_{j+1}^i \setminus \mathcal{K}_j^i = \{h = F_i(\hat{h}) \; : \; \hat{h} \in \nabla_j^{b(\Omega_i)}\} \tag{3.5}$$

through the relation

$$\psi_{j,h}^{(i)} \;:=\; \hat{\psi}_{j,\hat{h}} \circ G_i, \qquad \forall h \in \mathcal{H}_j^i, \quad h = F_i(\hat{h}). \tag{3.6}$$

The space $W_j(\Omega_i)$ and the similarly defined space $\tilde{W}_j(\Omega_i)$ form biorthogonal complements; the bases Ψ_j^i, and $\tilde{\Psi}_j^i$ are biorthogonal (with respect to $\langle\cdot,\cdot\rangle_{\Omega_i}$). It is easily seen that the dual multiresolution analyses on Ω_i defined in this way inherit the properties of the multiresolution analyses on $\hat{\Omega}$.

Finally, we introduce a concept that will be useful in the sequel. A point $h \in \mathcal{H}_j^i$ is termed *internal* to Ω_i if $h = F_i(\hat{h})$, with $\hat{h} = (\hat{h}_1, \cdots, \hat{h}_n)$ such that each component $\hat{h}_l$ belongs to $\Delta_j^{int} \cup \nabla_j^{int}$ (see (2.6)).

3.3. Multiresolution on the global domain. Now we describe the construction of dual multiresolution analyses on $\bar{\Omega}$. Let us define, for all $j \geq j_0$,

$$V_j(\Omega) := \{v \in C^0(\bar{\Omega}) : v_{|\Omega_i} \in V_j(\Omega_i),\, i = 1, \ldots, N\}; \tag{3.7}$$

the dual spaces $\tilde{V}_j(\Omega)$ are defined in a similar manner. In order to define a basis of $V_j(\Omega)$, let us introduce the set

$$\mathcal{K}_j := \bigcup_{i=1}^{N} \mathcal{K}_j^i \tag{3.8}$$

containing all the grid points in $\bar{\Omega}$. Each point of $\mathcal{K}_j$ can be associated to one single scale basis function of $V_j(\Omega)$, and conversely. To accomplish this, let us set

$$I(k) := \left\{ i \in \{1, \dots, N\} : k \in \bar{\Omega}_i \right\}, \quad \forall k \in \mathcal{K}_j,$$

as well as

$$\hat{k}^{(i)} := G_i(k), \quad \forall i \in I(k), \quad \forall k \in \mathcal{K}_j.$$

Then, for any $k \in \mathcal{K}_j$ let us define the function $\varphi_{j,k}$ as follows

$$\varphi_{j,k\,|\Omega_i} := \begin{cases} |I(k)|^{-1/2}\, \varphi^{(i)}_{j,k}, & \text{if } i \in I(k), \\ 0, & \text{otherwise.} \end{cases} \tag{3.9}$$

This function belongs to $V_j(\Omega)$, since it is continuous across the interelement boundaries (see [4], Section 4.2). Let us now set $\Phi_j := \{\varphi_{j,k} : k \in \mathcal{K}_j\}$. The dual family $\tilde{\Phi}_j := \{\tilde{\varphi}_{j,k} : k \in \mathcal{K}_j\}$ is defined as in (3.9), simply by replacing each $\varphi^{(i)}_{j,k}$ by $\tilde{\varphi}^{(i)}_{j,k}$. (For our B-spline example, matched scaling functions are displayed in Figures 4.1 and 5.2 in Sections 4 and 5, respectively.) Then, we have $V_j(\Omega) = \operatorname{span} \Phi_j$, $\tilde{V}_j(\Omega) = \operatorname{span} \tilde{\Phi}_j$. By defining the L^2 type inner product on Ω

$$\langle u, v \rangle_\Omega := \sum_{i=1}^{N} \langle u, v \rangle_{\Omega_i}, \tag{3.10}$$

it is easy to obtain the biorthogonality relations $\langle \varphi_{j,k}, \tilde{\varphi}_{j,k'} \rangle_\Omega = \delta_{k,k'}$, from those in each Ω_i.

3.4. Wavelets on the global domain. We now begin the construction of biorthogonal complement spaces $W_j(\Omega)$ and $\tilde{W}_j(\Omega)$ ($j \geq j_0$) for $V_{j+1}(\Omega)$ and $\tilde{V}_{j+1}(\Omega)$ as well as the corresponding biorthogonal bases Ψ_j and $\tilde{\Psi}_j$. Given the set of grid points

$$\mathcal{H}_j := \mathcal{K}_{j+1} \setminus \mathcal{K}_j =: \bigcup_{i=1}^{N} \mathcal{H}^i_j,$$

we shall associate to each $h \in \mathcal{H}_j$ a function $\psi_{j,h} \in W_j(\Omega)$ and a function $\tilde{\psi}_{j,h} \in \tilde{W}_j(\Omega)$. Then, we shall set $\Psi_j := \{\psi_{j,h} : h \in \mathcal{H}_j\}$, $\tilde{\Psi}_j := \{\tilde{\psi}_{j,h} : h \in \mathcal{H}_j\}$.

At first, let us observe that if $h \in \mathcal{H}^i_j$ is such that the associated local wavelet $\psi^{(i)}_{j,h}$ (defined in (3.6)) vanishes identically on $\partial\Omega_i \setminus \partial\Omega$, then the function

$$\psi_{j,h}(x) := \begin{cases} \psi^{(i)}_{j,h}(x), & \text{if } x \in \Omega_i, \\ 0, & \text{otherwise,} \end{cases} \tag{3.11}$$

will be the global wavelet associated to h. This situation occurs either when h is an internal point of Ω_i (recall the definition of internal point given at the end of the previous subsection), or when all non internal coordinates of h correspond to a physical boundary (see Figure 3.1).

The remaining wavelets will be obtained by matching suitable combinations of scaling functions and wavelets in contiguous domains. In each of the three coming sections, we shall detail the construction of the univariate, bivariate and trivariate matched wavelets, respectively. Precisely,

- in 1D, wavelets are matched across the interface between two contiguous subdomains (i.e., subintervals), see Section 4;
- in 2D, wavelets are matched around the common vertex of several subdomains (cross point), or across the common side between two subdomains, see Section 5;

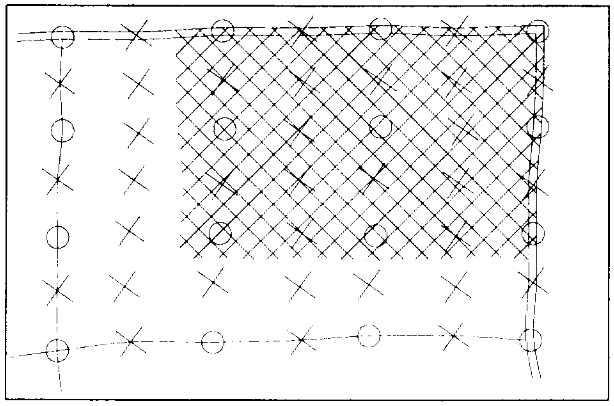

FIG. 3.1. *Scaling function grid points (circles) and wavelet grid points (crosses) in the subdomain Ω_i. The upper and right parts of the boundary of the subdomain belong to Γ. Wavelet grid points in the shaded area are associated to global wavelets constructed according to* (3.11).

- in 3D, wavelets are matched around cross points, or around a common edge of several subdomains, or across the common face of two subdomains, see Section 6.

Before going further on, let us make a general remark on vanishing moments. Wavelets on the reference domain satisfy the conditions

$$\int_{\hat\Omega} \hat x^r \hat\psi_{j,\hat h}(\hat x)\, d\hat x = 0, \qquad \forall \hat h, \ \ \forall |r| \le \tilde L - 1,$$

where $\hat x^r = (\hat x_1^{r_1}, \dots, \hat x_n^{r_n})$ and $|r| = \max_i r_i$; this follows from the fact that $\tilde V_j(\hat\Omega)$ contains the set $\mathcal{P}_{\tilde L-1}(\hat\Omega)$ of all polynomials of degree $\le \tilde L - 1$ in each space variable. Unless a very special mapping is used, similar conditions in Ω are not satisfied. However, they are replaced by analogous conditions, which still imply the compression property of wavelets. Indeed, $\tilde V_j(\Omega)$ contains the subspace

$$\mathcal{P}_{\tilde L-1}(\Omega) = \{p \in \mathcal{C}^0(\bar\Omega) \ : \ (p_{|\Omega_i})\hat{} \in \mathcal{P}_{\tilde L-1}(\hat\Omega), \ \forall i\},$$

so that one has

$$\langle p, \psi_{j,h}\rangle_\Omega = 0, \qquad \forall h \in \mathcal{H}_j, \ \ \forall p \in \mathcal{P}_{\tilde L-1}(\Omega).$$

A dual condition holds for the dual wavelets $\tilde\psi_{j,h}(x)$.

3.5. Characterization of Sobolev spaces. At the end of our construction we shall obtain a system of biorthogonal wavelets on Ω which allows the characterization of certain smoothness spaces. For instance, let us set

$$H_b^s(\Omega) := \{v \in H^s(\Omega) \ : \ v = 0 \text{ on } \Gamma_{\mathrm{Dir}}\} \tag{3.12}$$

for $s \in I\!N \setminus \{0\}$, and let us extend the definition by interpolation for $s \notin I\!N$, $s > 0$ (after setting $H_b^0(\Omega) = L^2(\Omega)$). Furthermore, we introduce another scale of Sobolev spaces, depending upon the partition $\mathcal{P} := \{\Omega_i : i = 1, \dots, N\}$ of Ω; precisely, we set

$$H_b^s(\Omega; \mathcal{P}) := \{v \in H_b^1(\Omega) \ : \ v_{|\Omega_i} \in H^s(\Omega_i), i = 1, \dots, N\} \tag{3.13}$$

for $s \in I\!N \setminus \{0\}$, equipped with the norm

$$\|v\|_{H_b^s(\Omega;\mathcal{P})} \ \sim \ \sum_{i=1}^N \|v_{|\Omega_i}\|_{H^s(\Omega_i)}, \qquad \forall v \in H_b^s(\Omega; \mathcal{P}),$$

and we extend the definition using interpolation for $s \notin I\!N$, $s > 0$ (again we set $H^0_b(\Omega;\mathcal{P}) = L^2(\Omega)$). The following Theorem summarizes the characterization features of our wavelet systems; they can be exploited in many different applications.

THEOREM 3.1. *([4], Theorem 5.6) Assume that $s \in [0, \min(L,\gamma))$. Then*

$$H^s_b(\Omega;\mathcal{P}) = \left\{ v \in L^2(\Omega) \ : \ \sum_{j=j_0}^{\infty} \sum_{h\in\mathcal{H}_j} 2^{2sj} \, |\langle v, \tilde{\psi}_{j,h}\rangle_\Omega|^2 < \infty \right\}.$$

In addition, if $v \in H^s_b(\Omega;\mathcal{P})$, then

$$v = \sum_{k\in\mathcal{K}_{j_0}} \langle v, \tilde{\varphi}_{j_0,k}\rangle_\Omega \, \varphi_{j_0,k} \ + \ \sum_{j=j_0}^{\infty} \sum_{h\in\mathcal{H}_j} \langle v, \tilde{\psi}_{j,h}\rangle_\Omega \, \psi_{j,h}, \tag{3.14}$$

the series being convergent in the norm of $H^s_b(\Omega;\mathcal{P})$, and

$$\|v\|^2_{H^s_b(\Omega;\mathcal{P})} \sim \sum_{k\in\mathcal{K}_{j_0}} 2^{2sj_0} \, |\langle v, \tilde{\varphi}_{j_0,k}\rangle_\Omega|^2 \ + \ \sum_{j=j_0}^{\infty} \sum_{h\in\mathcal{H}_j} 2^{2sj} \, |\langle v, \tilde{\psi}_{j,h}\rangle_\Omega|^2. \tag{3.15}$$

A dual statement holds if we exchange the roles of $V_j(\Omega)$ and $\tilde{V}_j(\Omega)$.

Moreover, if $s \in (-\min(\tilde{L},\tilde{\gamma}), 0)$, the formulas (3.14) and (3.15) hold for all $v \in H^s_b(\Omega;\mathcal{P}) := (H^{|s|}_b(\Omega;\mathcal{P}))'$, provided the inner product $\langle\cdot,\cdot\rangle_\Omega$ is replaced by the duality pairing between the spaces $H^s_b(\Omega;\mathcal{P})$ and $H^{|s|}_b(\Omega;\mathcal{P})$. □

4. Univariate matched wavelets and other functions. In this section, we describe the construction of matched wavelets and other functions in the one–dimensional case. Since this material will be used in the subsequent construction of higher dimensional wavelets, we restrict ourselves to the natural reference situation of the interval $I = (-1,1)$ divided in the two subintervals $I_- = (-1,0)$ and $I_+ = (0,1)$ by the interface point $C = 0$. It is straighforward to reduce any other one–dimensional matching to the present situation, by possibly introducing a suitable parametric mapping.

The scaling function $\hat{\varphi}_{j,0}$, associated to the interface point $C = 0$, is defined by

$$\hat{\varphi}_{j,0}(\hat{x}) := \frac{1}{\sqrt{2}} \begin{cases} \xi_{j,1}(\hat{x}+1), & \hat{x} \in I_-, \\ \xi_{j,0}(\hat{x}), & \hat{x} \in I_+. \end{cases} \tag{4.1}$$

Example (continued). *For our B-spline example, the function* (4.1) *and its dual are displayed in Figure 4.1.* □

4.1. Wavelets. Let us consider the local basis functions on each subdomain

$$\hat{\psi}^-_e(\hat{x}) := \begin{cases} \xi_{j,1}(\hat{x}+1), & e = 0, \\ \eta_{j,\nu_{j,M_j}}(\hat{x}+1), & e = 1, \end{cases} \qquad \hat{x} \in I_-,$$

$$\hat{\psi}^+_e(\hat{x}) := \begin{cases} \xi_{j,0}(\hat{x}), & e = 0, \\ \eta_{j,\nu_{j,1}}(\hat{x}), & e = 1, \end{cases} \qquad \hat{x} \in I_+,$$

and let us set (see [4], (5.6))

$$V^0_{j+1}(I_\pm) := \mathrm{span}\{\hat{\psi}^\pm_e \ : \ e \in \{0,1\}\}.$$

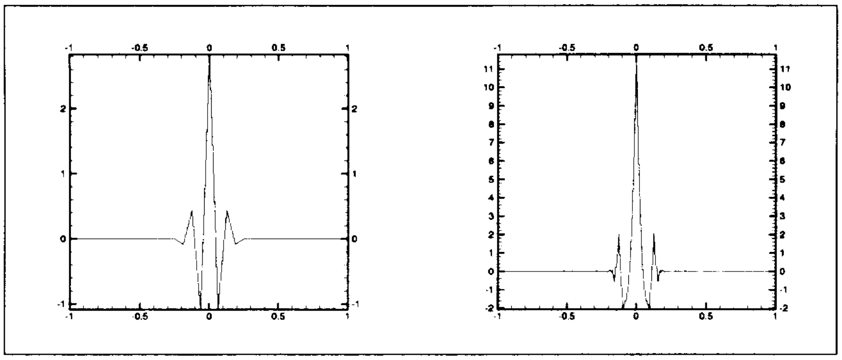

FIG. 4.1. *Matched primal and dual scaling functions at the cross point.*

Any function $v^{\pm} \in V^0_{j+1}(I_{\pm})$ can be written as $v^{\pm} = \sum_{e\in\{0,1\}} \alpha^{\pm}_e \hat{\psi}^{\pm}_e$; let us denote by $\boldsymbol{\alpha}^{\pm} := (\alpha^{\pm}_0, \alpha^{\pm}_1)$ the vectors of the local degrees of freedom. We want to build the local space

$$V^0_{j+1}(I) := \{v \in C^0(\bar{I}) \,:\, v_{|I_{\pm}} \in V^0_{j+1}(I_{\pm})\}$$

by matching functions in $V^0_{j+1}(I_-)$ and $V^0_{j+1}(I_+)$, and we want to find a basis for the subspace $W^0_j(I) := \{v \in V^0_{j+1}(I) : (v, \hat{\tilde{\varphi}}_{j,0})_{L^2(I)} = 0\}$. The matching condition between two functions $v^{\pm} \in V^0_{j+1}(I_{\pm})$ reads:

$$\alpha^-_0\, \xi_{j,1}(1) + \alpha^-_1\, \eta_{j,\nu_{j,M_j}}(1) = \alpha^+_0\, \xi_{j,0}(0) + \alpha^+_1\, \eta_{j,\nu_{j,1}}(0),$$

which, in view of the boundary values of the univariate scaling functions and wavelets (see (2.3-i.3)), is equivalent to

$$\alpha^-_0 + \alpha^-_1 = \alpha^+_0 + \alpha^+_1. \tag{4.2}$$

Next, we enforce the additional condition of orthogonality to $\hat{\tilde{\varphi}}_{j,0}$ which is expressed as

$$\begin{aligned} 0 &= \left(\alpha^-_0 \xi_{j,1}(\cdot+1) + \alpha^-_1 \eta_{j,\nu_{j,M_j}}(\cdot+1), \hat{\tilde{\varphi}}_{j,C_{|[-1,0]}}\right)_{L^2(-1,0)} \\ &\quad + \left(\alpha^+_0 \xi_{j,0}(\cdot) + \alpha^+_1 \eta_{j,\nu_{j,1}}(\cdot), \hat{\tilde{\varphi}}_{j,C_{|[0,1]}}\right)_{L^2(0,1)} \\ &= \frac{1}{\sqrt{2}}(\alpha^-_0 + \alpha^+_0), \end{aligned} \tag{4.3}$$

where the last equality is a consequence of the biorthogonality on the interval.

Using the matrix–vector notation of [4] (see formula (5.24) therein), condition (4.2) and condition (4.3) multiplied by $\sqrt{2}$ read

$$\boldsymbol{\mathcal{D}}\boldsymbol{\alpha} = \mathbf{0},$$

where

$$\boldsymbol{\mathcal{D}} := \begin{pmatrix} 1 & 1 & -1 & -1 \\ 1 & 0 & 1 & 0 \end{pmatrix}, \qquad \boldsymbol{\alpha} = (\boldsymbol{\alpha}^-, \boldsymbol{\alpha}^+)^t = (\alpha^-_0, \alpha^-_1, \alpha^+_0, \alpha^+_1)^t.$$

It is easily seen that $\boldsymbol{\mathcal{D}}\boldsymbol{\mathcal{D}}^t = \operatorname{diag}(4,2)$ is positive definite, so that $\boldsymbol{\mathcal{D}}$ has full rank 2. This implies that $\dim W^0_j(I) = 2$. It is directly seen that

$$\operatorname{Ker}\boldsymbol{\mathcal{D}} = \operatorname{span}\{(0,1,0,1)^t, (1,-1,-1,1)^t\}. \tag{4.4}$$

For the dual system, we have the same condition. So, it remains to find 2 particular choices of $\boldsymbol{\alpha} \in \operatorname{Ker} \boldsymbol{\mathcal{D}}$ and $\tilde{\boldsymbol{\alpha}} \in \operatorname{Ker} \tilde{\boldsymbol{\mathcal{D}}}$, i.e.,

$$\begin{aligned} \boldsymbol{\alpha}^l &:= a_{l,1}\,(0,1,0,1)^t + a_{l,2}\,(1,-1,-1,1)^t, \\ \tilde{\boldsymbol{\alpha}}^l &:= \tilde{a}_{l,1}\,(0,1,0,1)^t + \tilde{a}_{l,2}\,(1,-1,-1,1)^t, \end{aligned} \qquad l = 1,2,$$

that will define primal and dual wavelets $\hat{\psi}_j^l$, $\hat{\tilde{\psi}}_j^l$, $l = 1,2$, as

$$\hat{\psi}_j^l(\hat{x}) := \begin{cases} a_{l,2}\,\xi_{j,1}(\hat{x}+1) + (a_{l,1} - a_{l,2})\,\eta_{j,\nu_{j,M_j}}(\hat{x}+1), & \hat{x} \in \bar{I}_-, \\ -a_{l,2}\,\xi_{j,0}(\hat{x}) + (a_{l,1} + a_{l,2})\,\eta_{j,\nu_{j,1}}(\hat{x}), & \hat{x} \in \bar{I}_+. \end{cases} \tag{4.5}$$

The coefficients have to be chosen in order to obtain biorthogonal functions. Using the biorthogonality on the interval, it is readily seen that

$$\delta_{l,m} = (\hat{\psi}_j^l, \hat{\tilde{\psi}}_j^m)_{L^2(-1,1)} \;=\; 2\,a_{l,1}\tilde{a}_{m,1} + 4\,a_{l,2}\tilde{a}_{m,2}.$$

This can be rephrased by the matrix equation

$$\boldsymbol{Id} = \boldsymbol{A}\,\boldsymbol{X}\,\tilde{\boldsymbol{A}}^t, \tag{4.6}$$

where

$$\boldsymbol{A} := \begin{pmatrix} a_{1,1} & a_{1,2} \\ a_{2,1} & a_{2,2} \end{pmatrix}, \quad \tilde{\boldsymbol{A}} := \begin{pmatrix} \tilde{a}_{1,1} & \tilde{a}_{1,2} \\ \tilde{a}_{2,1} & \tilde{a}_{2,2} \end{pmatrix}, \quad \boldsymbol{X} := \begin{pmatrix} 2 & 0 \\ 0 & 4 \end{pmatrix}.$$

Since we have 4 equations for 8 unknowns, one can, in principle, choose 4 coefficients and the remaining 4 are then determined by (4.6).

It is convenient to relabel the wavelets $\hat{\psi}_j^l$, $\hat{\tilde{\psi}}_j^l$, $l = 1,2$, obtained by any particular choice of the coefficients as

$$\hat{\psi}_j^- := \hat{\psi}_j^1, \qquad \hat{\psi}_j^+ := \hat{\psi}_j^2, \tag{4.7}$$

(and similarly for the dual wavelets) so that they are associated in a natural way to the grid points $h_\pm \in \mathcal{H}_j$ located around C and defined as $h_+ := F_+(\nu_{j,1})$, $h_- := F_-(-1 + \nu_{j,M_j})$.

The above mentioned freedom in the construction can be used to fulfill additional features, which will now be described.

4.1.1. Additional features. Depending on the particular application one has in mind, one might need the basis functions to have some additional features such as, for example, zero values at the cross point, (skew-) symmetry and reflection invariance. We will now address these issues.

Zero values at the interface. The scaling and wavelet systems on the interval are supposed to be boundary adapted and boundary symmetric. Then, (4.5) implies

$$\hat{\psi}_j^l(0) = \lambda_j\,a_{1,l}, \quad \hat{\tilde{\psi}}_j^l(0) = \lambda_j\,\tilde{a}_{1,l}, \qquad \text{for } l = 1 \text{ or } l = 2,$$

where λ_j is defined in (2.3-j). Choosing these coefficients to be zero implies zero value of the corresponding wavelet function at the interface. Note that it is not possible to enforce the condition for $l = 1$ and $l = 2$ simultaneously, as this would contradict (4.6).

Symmetry and skew-symmetry. Let us assume that Ξ_j, $\tilde{\Xi}_j$ and Υ_j, $\tilde{\Upsilon}_j$ are reflection invariant. This implies in particular

$$\xi_{j,0}(\hat{x}) = \xi_{j,1}(1-\hat{x}), \qquad \eta_{j,\nu_{j,1}}(\hat{x}) = \eta_{j,\nu_{j,M_j}}(1-\hat{x}).$$

Then, we get, for $\hat{x} \in I$,

$$\begin{aligned} \hat{\psi}_j^{(a_1,a_2)}(-\hat{x}) &= \begin{cases} -a_2\,\xi_{j,1}(1+\hat{x}) + (a_1+a_2)\,\eta_{j,\nu_{j,M_j}}(1+\hat{x}), & \hat{x} \in I_-, \\ a_2\,\xi_{j,0}(\hat{x}) + (a_1-a_2)\,\eta_{j,\nu_{j,1}}(\hat{x}), & \hat{x} \in I_+, \end{cases} \\ &= \hat{\psi}_j^{(a_1,-a_2)}(\hat{x}), \end{aligned}$$

where the notation $\psi_j^{(a_1,a_2)}$ abbreviates that the function is associated to the vector (a_1,a_2). This implies

$$\hat{\psi}_j^l(-\hat{x}) = \begin{cases} -\hat{\psi}_j^l(\hat{x}), & \text{if } a_{l,1}=0, \\ \hat{\psi}_j^l(\hat{x}), & \text{if } a_{l,2}=0, \end{cases} \qquad \text{for } l=1 \text{ or } l=2,$$

so that we can choose one wavelet function to be either symmetric or skew-symmetric. The choice $\boldsymbol{A} = \begin{pmatrix} 0 & 1 \\ 1 & 0 \end{pmatrix}$ leads to one symmetric and one skew-symmetric wavelet. The dual wavelets are then defined by the matrix $\tilde{\boldsymbol{A}} = \begin{pmatrix} 0 & 1/4 \\ 1/2 & 0 \end{pmatrix}$ and have the same properties.

Reflection invariance. Under the same assumptions as before, the choice $\boldsymbol{A} = \begin{pmatrix} 1 & 1 \\ 1 & -1 \end{pmatrix}$ leads to primal wavelets that reflect into each other under the mapping $\hat{x} \mapsto -\hat{x}$. The dual wavelets are then defined by the matrix $\tilde{\boldsymbol{A}} = \begin{pmatrix} 1/4 & 1/8 \\ 1/4 & -1/8 \end{pmatrix}$, and have the same property.

Vanishing moments. Set, for a function f and a domain D,

$$M_r(f;D) = \int_D x^r\, f(x)\, dx.$$

Using the fact that the scaling functions in $[0,1]$ reproduce the constants, and exploiting the biorthogonality and the boundary adaptation property, it follows that

$$(1, \tilde{\xi}_{j,0})_{L^2(I_+)} = \lambda_j^{-1} = (1, \tilde{\xi}_{j,1}(\cdot+1))_{L^2(I_-)},$$

where again λ_j^{-1} is defined in (2.3-j); by similar arguments, we get

$$(x^r, \tilde{\xi}_{j,0})_{L^2(I_+)} = 0 = (x^r, \tilde{\xi}_{j,1}(\cdot+1))_{L^2(I_-)} \qquad 1 \le r \le L-1.$$

It is easily seen that these relations imply that the monomials x^r $(0 \le r \le L-1)$ restricted to the whole interval I belong to $V_j(I)$. Since the matched wavelets $\hat{\hat{\psi}}_j^l$ are orthogonal to $V_j(I)$, we conclude that

$$M_r(\hat{\hat{\psi}}_j^l; I) = 0, \quad 0 \le r \le L-1.$$

Dual relations hold for $\tilde{\psi}_j^l$. We conclude that the wavelet functions that arise by the matching procedure automatically have the same order of vanishing moments on the whole interval I as the original functions on the interval $[0,1]$.

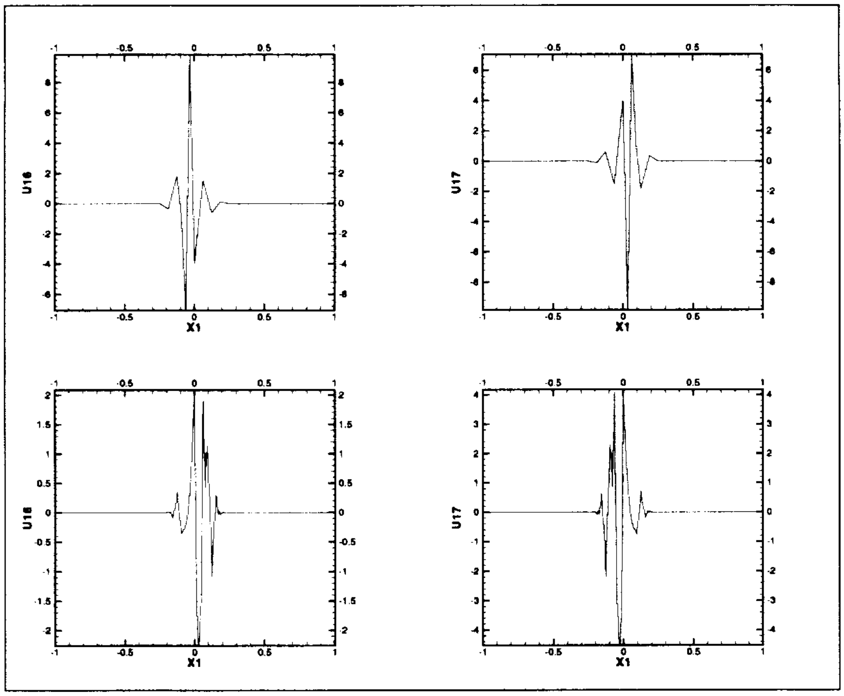

FIG. 4.2. *Matched primal and dual wavelets at the cross point.*

Support located in only one subdomain. It is readily seen that (4.5) implies that the arising wavelets are both located in both subdomains. It is not possible to localize them on only one side. However, since

$$\operatorname{diam}(\operatorname{supp} \eta_{j,h}) \sim \operatorname{diam}(\operatorname{supp} \tilde{\eta}_{j,h}) \sim 2^{-j},$$

one still has $\operatorname{diam}(\operatorname{supp} \psi_{j,h}) \sim 2^{-j}$ for $h = h_{\pm}$; the same property holds for the dual functions.

Example (continued). *For our B-spline example, matched wavelets defined in* (4.5) *with the choice of matrices $\boldsymbol{A}$ and $\tilde{\boldsymbol{A}}$ which guarantee reflection invariance (see above), are shown in Figure 4.2.* □

4.2. Another basis of matched functions. Now we aim at defining a basis of the local space $V^0_{j+1}(I)$. Compared to Subsection 4.1, the orthogonality condition (4.3) is missing, so that we obtain the following matching conditions in matrix-vector form

$$\boldsymbol{\mathcal{D}}\,\boldsymbol{\alpha} = \boldsymbol{0}, \qquad \text{with} \quad \boldsymbol{\mathcal{D}} := (1, 1, -1, -1), \qquad \boldsymbol{\alpha} = (\boldsymbol{\alpha}^-, \boldsymbol{\alpha}^+)^t = (\alpha_0^-, \alpha_1^-, \alpha_0^+, \alpha_1^+)^t.$$

It is obvious that $\operatorname{Ker} \boldsymbol{C} = \operatorname{span}\{(1,-1,0,0)^t, (0,0,1,-1)^t, (0,1,0,1)^t\}$ and we have to find 3 particular linear combinations, i.e.,

$$\begin{aligned} \boldsymbol{\alpha}^l &= a_{l,1}\,(1,-1,0,0)^t + a_{l,2}\,(0,0,1,-1)^t + a_{l,3}\,(0,1,0,1)^t, \\ \tilde{\boldsymbol{\alpha}}^l &= \tilde{a}_{l,1}\,(1,-1,0,0)^t + \tilde{a}_{l,2}\,(0,0,1,-1)^t + \tilde{a}_{l,3}\,(0,1,0,1)^t, \end{aligned} \qquad l = 1,2,3,$$

which give rise to the three basis functions

$$\hat{\vartheta}^l_j(\hat{x}) := \begin{cases} a_{l,1}\,\xi_{j,1}(\hat{x}) + (a_{l,3} - a_{l,1})\,\eta_{j,\nu_j,M_j}(\hat{x}), & \hat{x} \in I_-, \\ a_{l,2}\,\xi_{j,0}(\hat{x}) + (a_{l,3} - a_{l,2})\,\eta_{j,\nu_j,1}(\hat{x}), & \hat{x} \in I_+, \end{cases} \qquad l = 1,2,3, \tag{4.8}$$

In this case, the biorthogonality gives the conditions

$$\begin{aligned} \delta_{l,m} &= (\hat{\vartheta}^l_j, \hat{\tilde{\vartheta}}^m_j)_{L^2(-1,1)} \\ &= 2(a_{l,1}\tilde{a}_{m,1} + a_{l,2}\tilde{a}_{m,2} + a_{l,3}\tilde{a}_{m,3}) - a_{l,1}\tilde{a}_{m,3} - a_{l,3}\tilde{a}_{m,1} - a_{l,2}\tilde{a}_{m,3} - a_{l,3}\tilde{a}_{m,2}, \end{aligned}$$

which can be rewritten as $\boldsymbol{Id} = \boldsymbol{B}\,\boldsymbol{Y}\,\tilde{\boldsymbol{B}}^t$, where

$$\boldsymbol{B} := \begin{pmatrix} a_{1,1} & a_{1,2} & a_{1,3} \\ a_{2,1} & a_{2,2} & a_{2,3} \\ a_{3,1} & a_{3,2} & a_{3,3} \end{pmatrix}, \quad \tilde{\boldsymbol{B}} := \begin{pmatrix} \tilde{a}_{1,1} & \tilde{a}_{1,2} & \tilde{a}_{1,3} \\ \tilde{a}_{2,1} & \tilde{a}_{2,2} & \tilde{a}_{2,3} \\ \tilde{a}_{3,1} & \tilde{a}_{3,2} & \tilde{a}_{3,3} \end{pmatrix}, \quad \boldsymbol{Y} := \begin{pmatrix} 2 & 0 & -1 \\ 0 & 2 & -1 \\ -1 & -1 & 2 \end{pmatrix}.$$

After choosing one particular solution of this algebraic system, we relabel the functions as

$$\hat{\vartheta}_j^- := \hat{\vartheta}_j^1, \quad \hat{\vartheta}_j^0 := \hat{\vartheta}_j^2, \quad \hat{\vartheta}_j^+ := \hat{\vartheta}_j^3; \tag{4.9}$$

the dual functions are defined similarly.

4.2.1. Additional features. Additional features can be required to the functions $\hat{\vartheta}_j^l$, $l = 1, 2, 3$ just introduced.

Vanishing moments. In this case we have

$$M_r(\hat{\vartheta}_j^l; I) = (a_{l,1} + a_{l,2})\, M_r(\xi_{j,0}; I),$$

so that one preserves the order of vanishing moments if and only if $a_{l,1} = -a_{l,2}$.

Zero values at the cross point. Similarly to the results of Subsection 4.1, we obtain $\hat{\vartheta}_j^l(0) = a_{l,3}$ and $\hat{\tilde{\vartheta}}_j^l(0) = \tilde{a}_{l,3}$.

Symmetry of the arising functions. Using the same arguments as above, we obtain

$$\hat{\vartheta}_j^{(a_1,a_2,a_3)}(-\hat{x}) = \hat{\vartheta}_j^{(a_2,a_1,a_3)}(\hat{x}),$$

so that we have

$$\hat{\vartheta}_j^l(-\hat{x}) = \begin{cases} -\hat{\vartheta}_j^l(\hat{x}), & \text{if } a_{l,1} = -a_{l,2} \text{ and } a_{l,3} = 0, \\ \hat{\vartheta}_j^l(\hat{x}), & \text{if } a_{l,1} = a_{l,2}. \end{cases}$$

Support located in only one subdomain. Obviously, one has

$$\operatorname{supp} \hat{\vartheta}_j^l \subseteq \begin{cases} I_-, & \text{if } a_{l,2} = a_{l,3} = 0, \\ I_+, & \text{if } a_{l,1} = a_{l,3} = 0, \end{cases} \tag{4.10}$$

so that it is possible to construct 3 functions, such that only one of them is localized in both subdomains.

Example (continued). *We give one particular example of three functions, one located in I_-, one in I_+ and one in both subintervals. For the latter one, also the vanishing moment property is preserved. Let*

$$\boldsymbol{B} := \begin{pmatrix} 1 & 0 & 0 \\ 0 & 0 & 1 \\ 0 & 1 & 0 \end{pmatrix}. \tag{4.11}$$

It is readily seen that $\boldsymbol{B}^{-1} = \boldsymbol{B}^t$, hence we obtain the coefficients for the dual functions by

$$\tilde{\boldsymbol{B}} = \boldsymbol{B}\,\boldsymbol{Y}^{-t} = \begin{pmatrix} 3/4 & 1/4 & 1/2 \\ 1/2 & 1/2 & 1 \\ 1/4 & 3/4 & 1/2 \end{pmatrix}. \tag{4.12}$$

These particular functions are displayed in Figure 4.3. □

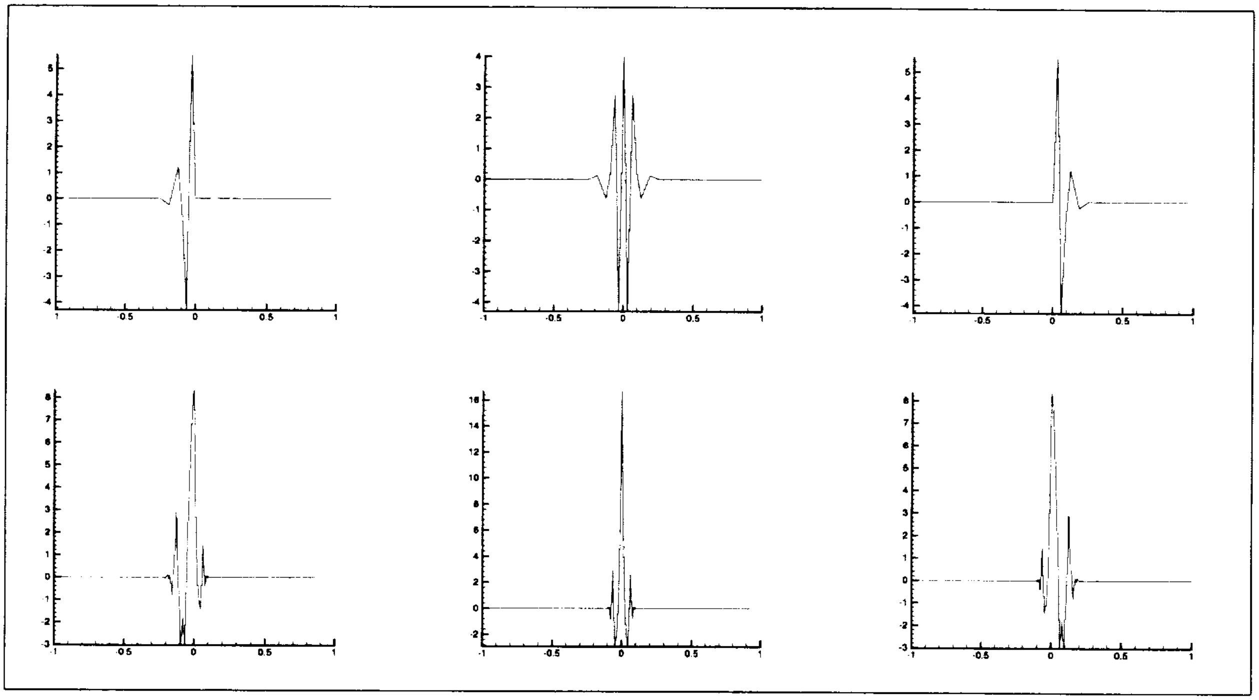

FIG. 4.3. *Primal and dual basis functions defined by* (4.11) *and* (4.12).

5. Bivariate matched wavelets. We shall now construct matched two-dimensional wavelets, by firstly considering an interior cross point, next a boundary cross point and finally the common side of two subdomains. In each case, we indicate how wavelets can be defined, which have the most localized support.

5.1. Matched wavelets around an interior cross point. We describe the construction of wavelets associated to grid points $h \in \mathcal{H}_j$ which are close to a cross point C, at which N_C subdomains meet. We assume that these subdomains are (re-)labeled by $\Omega_1, \ldots, \Omega_{N_C}$, in a counterclockwise order. Moreover, we set $\Gamma_{i,i+1} := \partial\Omega_i \cap \partial\Omega_{i+1}$. We start with the situation in which C is interior to Ω. In this case, it is convenient to set $\Omega_{N_C+1} := \Omega_1$.

At first, we deal with a particular choice of the mappings to the reference domain. Next, we shall show that all other possibilities can be easily reduced to this choice, which – therefore – can be thought of as a *reference situation.*

So, suppose that, for all $i \in \{1, \ldots, N_C\}$, one has $C = F_i(0,0)$ and $\Gamma_{i,i+1} = F_i(\hat{\sigma}_{01}) = F_{i+1}(\hat{\sigma}_{10})$, where $\hat{\sigma}_{01} := \{(0, \hat{x}_2) : 0 \le \hat{x}_2 \le 1\}$ and $\hat{\sigma}_{10} := \{(\hat{x}_1, 0) : 0 \le \hat{x}_1 \le 1\}$. The grid points surrounding C, to which we will associate the matched wavelets, are the $2N_C$ points $h_{C,l}$ defined as follows:

$$h_{C,2i-1} = F_i(\nu_{j,1}, \nu_{j,1}), \qquad h_{C,2i} = F_i(0, \nu_{j,1}), \qquad 1 \le i \le N_C. \tag{5.1}$$

Note that each evenly numbered point belongs to a side meeting at C, whereas each oddly numbered point is internal to a subdomain meeting at C (see Figure 5.1).

Dropping the index j, let us set

$$\psi_{00}^{(i)}(x) = \hat{\psi}_{00}(\hat{x}) = \xi_{j,0}(\hat{x}_1)\, \xi_{j,0}(\hat{x}_2),$$
$$\psi_{01}^{(i)}(x) = \hat{\psi}_{01}(\hat{x}) = \xi_{j,0}(\hat{x}_1)\, \eta_{j,\nu_{j,1}}(\hat{x}_2),$$

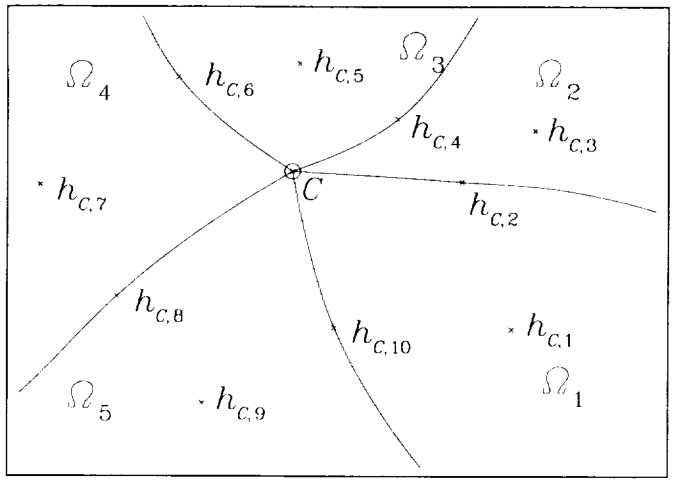

FIG. 5.1. *Grid points $h_{C,i}$, $i = 1, \dots, 10$, around a cross point C common to 5 subdomains.*

$$\psi_{10}^{(i)}(x) = \hat{\psi}_{10}(\hat{x}) = \eta_{j,\nu_{j,1}}(\hat{x}_1)\,\xi_{j,0}(\hat{x}_2),$$
$$\psi_{11}^{(i)}(x) = \hat{\psi}_{11}(\hat{x}) = \eta_{j,\nu_{j,1}}(\hat{x}_1)\,\eta_{j,\nu_{j,1}}(\hat{x}_2),$$

(see [4], formula (5.5)), as well as $V_{j+1}^C(\Omega_i) := \operatorname{span}\{\psi_e^{(i)} : e \in E^2\}$. A function $v^{(i)} \in V_{j+1}^C(\Omega_i)$ is written as

$$v^{(i)} = \sum_{e \in E^2} \alpha_e^{(i)}\,\psi_e^{(i)};$$

we shall introduce the column vector $\boldsymbol{\alpha}^{(i)} := (\alpha_e^{(i)})_{e \in E^2}$. In order to characterize the local space

$$V_{j+1}^C(\Omega) := \{v \in C^0(\bar{\Omega}) \,:\, v_{|\Omega_i} \in V_{j+1}^C(\Omega_i) \text{ if } i \in \{1, \dots, N_C\},\ v_{|\Omega_i} \equiv 0 \text{ elsewhere}\},$$

we proceed as in [4] (see Section 5.2), i.e., we enforce the continuity among the $v^{(i)}$ by considering the point C firstly, and the sides $\Gamma_{i,i+1}$, secondly. Recalling (2.3-i.3), the continuity at C yields the set of linearly independent conditions

$$\alpha_{00}^{(i)} + \alpha_{01}^{(i)} + \alpha_{10}^{(i)} + \alpha_{11}^{(i)} = \alpha_{00}^{(i+1)} + \alpha_{01}^{(i+1)} + \alpha_{10}^{(i+1)} + \alpha_{11}^{(i+1)}, \qquad 1 \le i \le N_C - 1, \tag{5.2}$$

or

$$\boldsymbol{c}_0 \cdot \boldsymbol{\alpha}^{(i)} = \boldsymbol{c}_0 \cdot \boldsymbol{\alpha}^{(i+1)}, \qquad 1 \le i \le N_C - 1,$$

with $\boldsymbol{c}_0 = (1,1,1,1)$. Denoting by $\boldsymbol{\alpha} := (\boldsymbol{\alpha}^{(i)})_{i=1,\dots,N_C} \in \mathbb{R}^{4N_C}$ the column vector of all degrees of freedom, these conditions can be written in matrix–vector form as

$$\boldsymbol{C}_0\,\boldsymbol{\alpha} = \boldsymbol{0}, \qquad \text{where} \qquad \boldsymbol{C}_0 = \begin{pmatrix} \boldsymbol{c}_0 & -\boldsymbol{c}_0 & & \\ & \ddots & \ddots & \\ & & \boldsymbol{c}_0 & -\boldsymbol{c}_0 \end{pmatrix} \in \mathbb{R}^{(N_C-1)\times 4N_C}.$$

Let us now enforce continuity along the sides $\Gamma_{i,i+1}$. To this end, observe that

$$\begin{aligned} v_{|\Gamma_{i,i+1}}^{(i)}(x) &= \lambda_j\Big((\alpha_{00}^{(i)} + \alpha_{10}^{(i)})\xi_{j,0}(\hat{x}_2) + (\alpha_{01}^{(i)} + \alpha_{11}^{(i)})\eta_{j,\nu_{j,1}}(\hat{x}_2)\Big), \\ v_{|\Gamma_{i,i+1}}^{(i+1)}(x) &= \lambda_j\Big((\alpha_{00}^{(i+1)} + \alpha_{01}^{(i+1)})\xi_{j,0}(\hat{x}_1) + (\alpha_{10}^{(i+1)} + \alpha_{11}^{(i+1)})\eta_{j,\nu_{j,1}}(\hat{x}_1)\Big), \end{aligned} \tag{5.3}$$

with λ_j defined in (2.3-j). Because of the linear independence of the univariate functions, the matching is equivalent to

$$\begin{aligned} \alpha_{00}^{(i)} + \alpha_{10}^{(i)} &= \alpha_{00}^{(i+1)} + \alpha_{01}^{(i+1)}, \\ \alpha_{01}^{(i)} + \alpha_{11}^{(i)} &= \alpha_{10}^{(i+1)} + \alpha_{11}^{(i+1)}. \end{aligned} \tag{5.4}$$

Since we have already enforced the continuity at $C \in \Gamma_{i,i+1}$ (see (5.2)), it is enough to require that a particular linear combination of the latter equations holds; precisely, we enforce

$$\alpha_{00}^{(i)} - \alpha_{01}^{(i)} + \alpha_{10}^{(i)} - \alpha_{11}^{(i)} = \alpha_{00}^{(i+1)} + \alpha_{01}^{(i+1)} - \alpha_{10}^{(i+1)} - \alpha_{11}^{(i+1)}$$

(for details, see [4], Proposition 5.2). Introducing the vectors $\boldsymbol{c}' = (1,-1,1,-1)$ and $\boldsymbol{c}'' = (1,1,-1,-1)$, these conditions can be rephrased as

$$\mathcal{C}_1\,\boldsymbol{\alpha} = \boldsymbol{0}, \qquad \text{where} \qquad \mathcal{C}_1 = \begin{pmatrix} \boldsymbol{c}' & -\boldsymbol{c}'' & & \\ & \ddots & \ddots & \\ & & \boldsymbol{c}' & -\boldsymbol{c}'' \\ -\boldsymbol{c}'' & & & \boldsymbol{c}' \end{pmatrix} \in \mathbb{R}^{N_C \times 4N_C}. \tag{5.5}$$

We are interested in finding a basis for the subspace $W_j^C(\Omega) := \{v \in V_{j+1}^C(\Omega) : \langle v, \tilde{\varphi}_{j,C}\rangle_\Omega = 0\}$. Recalling that, by (3.9),

$$\tilde{\varphi}_{j,C|\Omega_i}(x) = \frac{1}{\sqrt{N_C}}\,(\tilde{\xi}_{j,0} \otimes \tilde{\xi}_{j,0})(\hat{x}), \quad \hat{x} = G_i(x),\ i = 1,\ldots,N_C,$$

we obtain the condition

$$\sum_{i=1}^{N_C} \alpha_{00}^{(i)} = 0.$$

So, introducing the vector $\boldsymbol{b} := (1,0,0,0)$, all conditions enforced so far can be summarized in

$$\mathcal{D}\,\boldsymbol{\alpha} = \boldsymbol{0}, \qquad \text{where} \qquad \mathcal{D} = \begin{bmatrix} \mathcal{C}_0 \\ \mathcal{C}_1 \\ \mathcal{B} \end{bmatrix} \in \mathbb{R}^{2N_C \times 4N_C}, \qquad \mathcal{B} := (\boldsymbol{b},\ldots,\boldsymbol{b}) \in \mathbb{R}^{1\times 4N_C}.$$

It can easily be seen that

$$\mathcal{D}\mathcal{D}^t = \left[\begin{array}{ccccc|ccc|c} 8 & -4 & & & 0 & & & & \\ -4 & 8 & -4 & & & & & & \\ & \ddots & \ddots & \ddots & & & & & \\ & & \ddots & \ddots & -4 & & & & \\ 0 & & & -4 & 8 & & & & \\ \hline & & & & & 8 & & & \\ & & & & & & \ddots & & \\ & & & & & & & 8 & \\ \hline & & & & & & & & N_C \end{array}\right] \in \mathbb{R}^{2N_C \times 2N_C};$$

the evident symmetric positive definite character of $\mathcal{D}\mathcal{D}^t$ means that $\mathcal{D}$ has full rank. This implies the existence of exactly $2N_C$ linearly independent functions in $W_j^C(\Omega)$, i.e., $\dim W_j^C(\Omega) = 2N_C$. The parallel construction for $\tilde{W}_j^C(\Omega)$ leads to the condition $\boldsymbol{\mathcal{D}}\,\tilde{\boldsymbol{\alpha}} = \mathbf{0}$ (note that the matrix $\boldsymbol{\mathcal{D}}$ is the same as for the primal system). Finally, we enforce biorthogonality between the primal and dual basis functions determined in this way. To this end, we choose a basis $\{\boldsymbol{\kappa}_1, \ldots, \boldsymbol{\kappa}_{2N_C}\}$ in $\operatorname{Ker}\boldsymbol{\mathcal{D}}$, and we look for linear combinations of these vectors

$$\boldsymbol{\alpha}^l = \sum_{m=1}^{2N_C} a_{l,m}\,\boldsymbol{\kappa}_m, \qquad \tilde{\boldsymbol{\alpha}}^l = \sum_{m=1}^{2N_C} \tilde{a}_{l,m}\,\boldsymbol{\kappa}_m, \qquad 1 \le l \le 2N_C,$$

such that, if $\boldsymbol{\alpha}^l$ is decomposed as $(\boldsymbol{\alpha}^{l,(i)})_{i=1,\ldots,2N_C}$, the corresponding wavelets

$$\psi_{j,C}^l(x) := \begin{cases} \sum_{e\in E^2} \alpha_e^{l,(i)}\,\hat{\psi}_e(\hat{x}), & \text{if } x \in \Omega_i,\ 1 \le i \le N_C, \\ 0, & \text{elsewhere,} \end{cases}$$

and the dual ones $\tilde{\psi}_{j,C}^l$ defined in a similar manner, form a biorthogonal system. Then, setting $\boldsymbol{\mathcal{K}} := (\boldsymbol{\kappa}_m)_{m=1,\ldots,2N_C}$, $\boldsymbol{A} := (a_{l,m})_{l,m=1,\ldots,2N_C}$, $\tilde{\boldsymbol{A}} := (\tilde{a}_{l,m})_{l,m=1,\ldots,2N_C}$, and $\boldsymbol{\mathcal{A}} := (\boldsymbol{\alpha}^l)_{l=1,\ldots,2N_C} = \boldsymbol{\mathcal{K}}\boldsymbol{A}^t$, $\tilde{\boldsymbol{\mathcal{A}}} := (\tilde{\boldsymbol{\alpha}}^l)_{l=1,\ldots,2N_C} = \boldsymbol{\mathcal{K}}\tilde{\boldsymbol{A}}^t$, and exploiting the biorthogonality property in each subdomain, we can express the biorthogonality condition in the form $\boldsymbol{\mathcal{A}}^t\,\tilde{\boldsymbol{\mathcal{A}}} = \boldsymbol{Id}$, i.e.,

$$\boldsymbol{A}\boldsymbol{\mathcal{K}}^t\boldsymbol{\mathcal{K}}\tilde{\boldsymbol{A}}^t = \boldsymbol{Id}. \tag{5.6}$$

Since $\boldsymbol{\mathcal{K}}$ obviously has full rank, $\boldsymbol{\mathcal{K}}^t\boldsymbol{\mathcal{K}}$ is regular, so this matrix equation has a solution. In particular, one can choose $\boldsymbol{A} = \boldsymbol{Id}$ and consequently $\tilde{\boldsymbol{A}} = (\boldsymbol{\mathcal{K}}^t\boldsymbol{\mathcal{K}})^{-1}$. In Subsection 5.1.1, we shall exhibit a specific basis in $\operatorname{Ker}\boldsymbol{\mathcal{D}}$, which allows to obtain primal wavelets with minimal support around C.

Once the biorthogonal wavelets $\psi_{j,C}^l$ and $\tilde{\psi}_{j,C}^l$ ($1 \le l \le 2N_C$) have been determined, they can be associated to the $2N_C$ grid points $h_{C,l}$ surrounding C, defined in (5.1).

Reduction to the reference situation. Let us now show that we can reduce any interior cross point situation to the one described above. To this end, let us consider any subdomain Ω_i having C as a vertex. Then, we have the following 4 cases:

a) $C = F_i(0,0)$, b) $C = F_i(1,1)$,

c) $C = F_i(0,1)$, d) $C = F_i(1,0)$.

Recalling the assumption $\det(JF_i) > 0$ in (3.1), it follows that in cases a) and b) the indices of the frozen coordinates of $\hat{\Gamma}_{i-1,i}$ and $\hat{\Gamma}_{i,i+1}$ are given by $\mathcal{L}_{\hat{\Gamma}_{i-1,i}} = \{2\}$, $\mathcal{L}_{\hat{\Gamma}_{i,i+1}} = \{1\}$, whereas in cases c) and d) one has $\mathcal{L}_{\hat{\Gamma}_{i-1,i}} = \{1\}$, $\mathcal{L}_{\hat{\Gamma}_{i,i+1}} = \{2\}$. It is straightforward to see that the matching conditions along $\Gamma_{i-1,i}$ and $\Gamma_{i,i+1}$ in cases a) and b) yield the same vectors $\boldsymbol{c}'$ and $\boldsymbol{c}''$ defined above, whereas the roles of these vectors are interchanged in the remaining cases.

If $\boldsymbol{\alpha}^{(i)} = (\alpha_{00}^{(i)}, \alpha_{01}^{(i)}, \alpha_{10}^{(i)}, \alpha_{11}^{(i)})^t$, let us denote by $\check{\boldsymbol{\alpha}}^{(i)} := (\alpha_{00}^{(i)}, \alpha_{10}^{(i)}, \alpha_{01}^{(i)}, \alpha_{11}^{(i)})^t$ the modified vector and by $\check{\boldsymbol{\mathcal{D}}}$ the matrix obtained by modifying $\boldsymbol{\mathcal{D}}$ according to cases c) and d). Since it is readily seen that $\boldsymbol{c}_0 \cdot (\boldsymbol{c}')^t = \boldsymbol{c}_0 \cdot (\boldsymbol{c}'')^t = 0$, $\boldsymbol{b} \cdot (\boldsymbol{c}')^t = \boldsymbol{b} \cdot (\boldsymbol{c}'')^t = 0$, $\boldsymbol{c}' \cdot \boldsymbol{\alpha}^{(i)} = \boldsymbol{c}'' \cdot \check{\boldsymbol{\alpha}}^{(i)}$ as well as $\boldsymbol{c}'' \cdot \boldsymbol{\alpha}^{(i)} = \boldsymbol{c}' \cdot \check{\boldsymbol{\alpha}}^{(i)}$, we obtain, as desired, $\boldsymbol{\mathcal{D}}\,\boldsymbol{\alpha} = \check{\boldsymbol{\mathcal{D}}}\,\check{\boldsymbol{\alpha}}$.

This procedure can be applied to all subdomains meeting at C, and so we are back to the *reference situation.*

The biorthogonalization is performed following the same guidelines described above; obviously, the definition of the wavelets and the associated grid points has to be adapted to the specific orientation of the mappings to the reference domain.

5.1.1. Wavelets with minimal support. The perhaps most important feature, in view of numerical applications, is a minimal support of the wavelets, since this implies minimal length of the corresponding filters.

Let us first consider under which circumstances it is possible to construct wavelets that are supported in only one subdomain Ω_i. By the matching at the cross point and the sides, we obtain the three conditions

$$\boldsymbol{c}_0 \cdot \boldsymbol{\alpha}^{(i)} = \boldsymbol{c}' \cdot \boldsymbol{\alpha}^{(i)} = \boldsymbol{c}'' \cdot \boldsymbol{\alpha}^{(i)} = 0. \tag{5.7}$$

It is readily seen that the vectors $(a, -a, -a, a)$, for some $a \in \mathbb{R}$, are the only solutions of (5.7). Thus, any function defined as

$$\psi(x) := \begin{cases} a\hat{\psi}_{00}(\hat{x}) - a\hat{\psi}_{01}(\hat{x}) - a\hat{\psi}_{10}(\hat{x}) + a\hat{\psi}_{11}(\hat{x}), & x \in \Omega_i, \\ 0, & \text{elsewhere,} \end{cases} \tag{5.8}$$

belongs to $V_{j+1}^C(\Omega)$ and is supported only in Ω_i. However, such a function cannot be a wavelet because, by imposing the orthogonality to $\tilde{\varphi}_{j,C}$, one gets the extra condition $\boldsymbol{b} \cdot \boldsymbol{\alpha}^{(i)} = \alpha_{00}^{(i)} = a = 0$. This implies that it is not possible to have wavelets supported in only one subdomain. On the contrary, we are going to show that it is possible to construct $2N_C - 1$ out of $2N_C$ wavelets to be supported in only two contiguous subdomain. To this end, let us deal with subdomains Ω_i and Ω_{i+1}. Considering the block structure of the matrix $\boldsymbol{\mathcal{D}}$, the corresponding vectors of coefficients $\boldsymbol{\alpha}^{(i)}$, $\boldsymbol{\alpha}^{(i+1)}$ have to fulfill the local equation

$$\begin{bmatrix} \boldsymbol{c}_0 & -\boldsymbol{c}_0 \\ \boldsymbol{c}' & -\boldsymbol{c}'' \\ \boldsymbol{b} & \boldsymbol{b} \end{bmatrix} \begin{bmatrix} \boldsymbol{\alpha}^{(i)} \\ \boldsymbol{\alpha}^{(i+1)} \end{bmatrix} = \mathbf{0}.$$

It is easily seen that the two linearly independent vectors

$$(\boldsymbol{\alpha}^{1,(i)}, \boldsymbol{\alpha}^{1,(i+1)}) := (0, 0, -1, 1, 0, -1, 0, 1)^t, \quad (\boldsymbol{\alpha}^{2,(i)}, \boldsymbol{\alpha}^{2,(i+1)}) := (-1, 1, 0, 0, 1, -2, -1, 2)^t$$

solve this equation. Setting all the remaining coefficients in $\boldsymbol{\alpha}$ to zero leads to the two seeked wavelet functions.

We observe that one out of these $2N_C$ functions is linearly dependent on all the others: since all these functions vanish at C, there are at most $(2N_C - 1)$ linearly independent functions among them. On the other hand, we now show that the following $2N_C$ functions are linearly independent:

$$\psi_{j,C}^l(x) := \begin{cases} \sum_{e \in E^2} \alpha_e^{1,(i)} \, \hat{\psi}_e(\hat{x}), & x \in \Omega_i, \\ \sum_{e \in E^2} \alpha_e^{1,(i+1)} \, \hat{\psi}_e(\hat{x}), & x \in \Omega_{i+1}, \\ 0, & \text{elsewhere,} \end{cases} \tag{5.9}$$

for $l = 2i - 1$, $i \in \{1, \dots, N_C\}$,

$$\psi_{j,C}^l(x) := \begin{cases} \sum_{e \in E^2} \alpha_e^{2,(i)} \, \hat{\psi}_e(\hat{x}), & x \in \Omega_i, \\ \sum_{e \in E^2} \alpha_e^{2,(i+1)} \, \hat{\psi}_e(\hat{x}), & x \in \Omega_{i+1}, \\ 0, & \text{elsewhere,} \end{cases} \tag{5.10}$$

for $l = 2i$, $i \in \{1, \dots, N_C - 1\}$, and

$$\psi_{j,C}^{2N_C}(x) := \psi_{j,C}^{\text{glob}}(x) := \begin{cases} \hat{\psi}_{11}(\hat{x}), & x \in \Omega_i,\ 1 \le i \le N_C, \\ 0, & \text{elsewhere.} \end{cases} \tag{5.11}$$

Indeed, if $\psi := \sum_{m=1}^{2N_C} \lambda_m \, \psi_{j,C}^m \equiv 0$, then $\psi(C) = 0$ implies $\lambda_{2N_C} = 0$ and $\psi_{|\Gamma_{N_C,1}} \equiv 0$ implies $\lambda_{2N_C-1} = 0$. Then $\psi_{|\Omega_1} \equiv 0$ implies $\lambda_1 \, \psi_{j,C}^1 + \lambda_2 \, \psi_{j,C}^2 \equiv 0$, which in turns implies $\lambda_1 = \lambda_2 = 0$. Considering in sequence $\Omega_2, \ldots, \Omega_{N_C-1}$ shows that all the coefficients must vanish.

Note that the primal basis we have just exhibited corresponds to choosing the following basis in $\operatorname{Ker} \boldsymbol{\mathcal{D}}$

$$
\begin{array}{lll}
\boldsymbol{\kappa}_m & := (\mathbf{0}, \ldots, \mathbf{0}, (\boldsymbol{\alpha}^{1,(i)})^t, (\boldsymbol{\alpha}^{1,(i+1)})^t, \mathbf{0}, \ldots, \mathbf{0})^t, & \text{if } m = 2i-1, \; i \in \{1, \ldots, N_C\}, \\
\boldsymbol{\kappa}_m & := (\mathbf{0}, \ldots, \mathbf{0}, (\boldsymbol{\alpha}^{2,(i)})^t, (\boldsymbol{\alpha}^{2,(i+1)})^t, \mathbf{0}, \ldots, \mathbf{0})^t, & \text{if } m = 2i, \; i \in \{1, \ldots, N_C - 1\}, \\
\boldsymbol{\kappa}_{2N_C} & := (\boldsymbol{d}, \cdots, \boldsymbol{d})^t & \text{with } \boldsymbol{d} = (0,0,0,1),
\end{array}
$$

and to choosing $\boldsymbol{A} = \boldsymbol{Id}$ in (5.6). Then the dual matrix $\tilde{\boldsymbol{A}}$ is given by $\tilde{\boldsymbol{A}} = (\boldsymbol{\mathcal{K}}^t \boldsymbol{\mathcal{K}})^{-1}$, where

$$
\boldsymbol{\mathcal{K}}^t \boldsymbol{\mathcal{K}} = \left[
\begin{array}{cc|cc|ccccc|cc|cc}
4 & 4 & 1 & -1 & & & & & & & & 1 & 2 \\
4 & 12 & 3 & -3 & & & & & & & & -1 & 2 \\
\hline
1 & 3 & \ddots & & \ddots & & & & & & & & 2 \\
-1 & -3 & & \ddots & & \ddots & & & & & & & \vdots \\
 & & \ddots & & \ddots & & \ddots & & & & & & \vdots \\
 & & & \ddots & & \ddots & & \ddots & & & & & \vdots \\
 & & & & \ddots & & \ddots & & & 1 & -1 & & \vdots \\
 & & & & & \ddots & & \ddots & & 3 & -3 & & 2 \\
\hline
 & & & & & & & 1 & 3 & 4 & 4 & 1 & 2 \\
 & & & & & & & -1 & -3 & 4 & 12 & 3 & 2 \\
\hline
1 & -1 & & & & & & & & 1 & 3 & 4 & 2 \\
2 & 2 & 2 & \cdots & \cdots & \cdots & \cdots & \cdots & 2 & 2 & 2 & 2 & N_C
\end{array}
\right]
$$

Example (continued). *We consider the situation in which four subdomains $\Omega_1, \ldots, \Omega_4$ meet at C (for simplicity, we assume linear parametric mappings from each subdomain to the reference domain). For our B-spline example, we show in Figure 5.2 the matched scaling function and the three different types of wavelets associated to grid points around C.* □

5.1.2. Tensor products of matched univariate functions. A common situation for an internal cross point is the case $N_C = 4$, i.e., four subdomains meeting at C. In such a geometry, it is easy to construct a basis for $W_j^C(\Omega)$ by properly tensorising the univariate matched functions defined in Section 4.

First of all, let us note that, by possibly introducing appropriate parametric mappings, we can reduce ourselves to the situation in which each subdomain is the image of one of the subdomains $I_\pm \times I_\pm$ (we use here the notation set at the beginning of Section 4), and C is the image of $\hat{C} = (0,0)$. Then, let us consider the set of univariate functions given by the scaling function $\hat{\varphi}_{j,0}$ defined in (4.1), the wavelets $\hat{\psi}_j^l$ defined in (4.5)–(4.7) and the functions $\hat{\vartheta}_j^l$ defined in (4.8)–(4.9). A basis in $W_j^C(\Omega)$ is obtained by taking the image of 8 linearly independent tensor products of such functions satisfying the condition of orthogonality to the dual scaling function $\hat{\tilde{\varphi}}_{j,0} = \hat{\tilde{\varphi}}_{j,0} \otimes \hat{\tilde{\varphi}}_{j,0}$. For example, a possible choice is

$$
\begin{array}{ccc}
\hat{\psi}_j^- \otimes \hat{\vartheta}_j^+, & \hat{\varphi}_{j,0} \otimes \hat{\psi}_j^+, & \hat{\psi}_j^+ \otimes \hat{\vartheta}_j^+, \\
\hat{\psi}_j^- \otimes \hat{\vartheta}_j^0, & & \hat{\psi}_j^+ \otimes \hat{\vartheta}_j^0, \\
\hat{\psi}_j^- \otimes \hat{\vartheta}_j^-, & \hat{\varphi}_{j,0} \otimes \hat{\psi}_j^-, & \hat{\psi}_j^+ \otimes \hat{\vartheta}_j^-,
\end{array}
$$

(obviously, these functions are extended by zero outside the union of the four subdomains) whose association to the 8 wavelet grid points around C is self evident. Note that this construction does not necessarily require

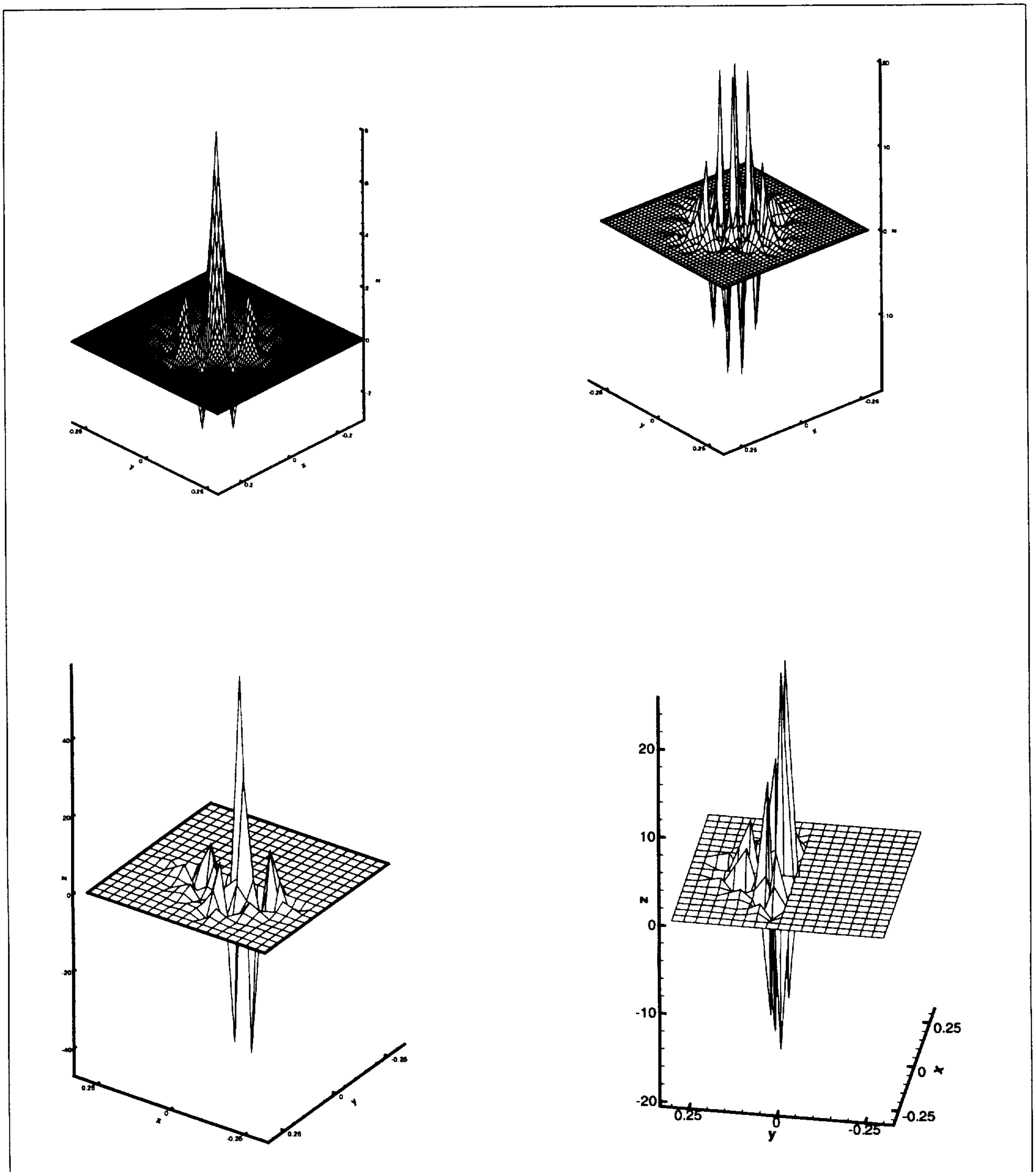

FIG. 5.2. *Matched scaling function (1st row) and primal wavelets $\psi^m_{j,C}$. In the first row the wavelet $\psi^8_{j,C}$ is displayed. The second row shows the functions $\psi^1_{j,C}$ and $\psi^2_{j,C}$ that are supported in Ω_1 and Ω_2. The remaining 5 wavelets are rotations of these two functions. (Note that only a portion of each subdomain around C is shown.)*

the functions $\hat{\vartheta}^l_j$ to have minimal support in the sense of (4.10), although efficiency will be enhanced by this feature.

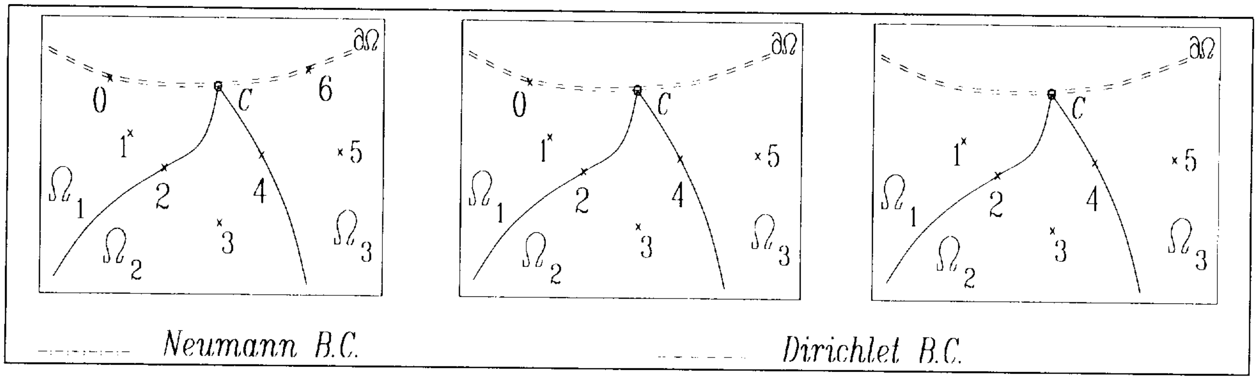

FIG. 5.3. *Grid points $h_{C,i}$ (labeled only by i) around a boundary cross point in the 3 different cases (from left to right: pure Neumann, mixed and pure Dirichlet case).*

5.2. Matched wavelets around a boundary cross point. Let us now consider the situation in which $C \in \partial\Omega$ is common to N_C subdomains $\Omega_1, \dots, \Omega_{N_C}$ ordered counterclockwise. We assume that Ω_1 (Ω_{N_C}, resp.) has a side, termed Γ_1 (Γ_{N_C}, resp.), which contains C and lies on $\partial\Omega$. Then, the following cases may occur:

a) $\Gamma_1, \Gamma_{N_C} \in \Gamma_{\text{Neu}}$

b) $\Gamma_1 \in \Gamma_{\text{Dir}}, \Gamma_{N_C} \in \Gamma_{\text{Neu}}$ c) $\Gamma_1 \in \Gamma_{\text{Neu}}, \Gamma_{N_C} \in \Gamma_{\text{Dir}}$

d) $\Gamma_1, \Gamma_{N_C} \in \Gamma_{\text{Dir}}$.

Since all arguments concerning biorthogonalization carry over from the interior cross point case, in the sequel we will only detail the matching and orthogonality conditions for each case separately.

Pure Neumann case. Let us start by considering case a). The matching at the cross point C only differs from the interior cross point case by the absence of a matching condition between Ω_1 and Ω_{N_C}. However, in the interior case, this condition turned out to be linearly dependent on the other ones, hence, there was no need to explicitly enforce it. This implies that the matrices describing the matching at C are the same: $\boldsymbol{\mathcal{C}}_0^{\text{Neu}} = \boldsymbol{\mathcal{C}}_0$.

The matching conditions along the sides are the same as well, with the only difference that now the last row in (5.5) is missing:

$$\boldsymbol{\mathcal{C}}_1^{\text{Neu}} = \begin{pmatrix} \boldsymbol{c}' & -\boldsymbol{c}'' & & \\ & \ddots & \ddots & \\ & & \boldsymbol{c}' & -\boldsymbol{c}'' \end{pmatrix} \in \mathbb{R}^{(N_C-1)\times 4N_C}.$$

Since $C \in \Gamma_{\text{Neu}}$, we observe that there exists a dual scaling function $\tilde{\varphi}_{j,C}$ associated to C. Consequently, we have to enforce orthogonality to this function, so we end up with the set of conditions

$$\boldsymbol{\mathcal{D}}^{\text{Neu}}\boldsymbol{\alpha} = \boldsymbol{0}, \qquad \text{with} \quad \boldsymbol{\mathcal{D}}^{\text{Neu}} = \begin{bmatrix} \boldsymbol{\mathcal{C}}_0 \\ \boldsymbol{\mathcal{C}}_1^{\text{Neu}} \\ \boldsymbol{\mathcal{B}} \end{bmatrix} \in \mathbb{R}^{(2N_C-1)\times 4N_C}.$$

As above, it is easily seen that $\boldsymbol{\mathcal{D}}^{\text{Neu}}$ has full rank; this implies that $\dim W_j^C(\Omega) = 2N_C + 1$. This is precisely the number of grid points surrounding C to which these wavelets can be associated; in the reference situation, they are the points (5.1) and the point $h_{C,0} := F_1(\nu_{j,1}, 0)$ (see Figure 5.3, left).

Mixed Neumann/Dirichlet case. Obviously, the mixed Neumann/Dirichlet cases b) and c) can be viewed as symmetric ones, so we will only detail case b) here. Since $C \in \bar{\Gamma}_{\text{Dir}}$, all functions in $V_{j+1}^C(\Omega)$ have to vanish at C. This means that we have to add one more condition to those posed at C, i.e., we obtain the matrix

$$\mathcal{C}_0^{\text{Mix}} = \begin{pmatrix} -\boldsymbol{c}_0 & & & & \\ \boldsymbol{c}_0 & -\boldsymbol{c}_0 & & & \\ & \ddots & \ddots & & \\ & & & \boldsymbol{c}_0 & -\boldsymbol{c}_0 \end{pmatrix} \in \mathbb{R}^{N_C \times 4N_C}.$$

Furthermore, again we assume to be in the reference situation described above, which implies that $\mathcal{L}_{\hat{\Gamma}_1} = \{2\}$ and $\mathcal{L}_{\hat{\Gamma}_{1,2}} = \{1\}$ for the domain Ω_1, i.e., the second coordinate of $\hat{\Gamma}_1$ is frozen. Let us consider a function $v^{(1)} \in V_{j+1}^C(\Omega_1)$, which is written as

$$v^{(1)}(x) = \sum_{e \in E^2} \alpha_e^{(1)} \hat{\psi}_e(\hat{x}), \qquad x \in \Omega_1.$$

Observing that

$$v^{(1)}_{|\Gamma_1}(x) = \lambda_j \left((\alpha_{00}^{(1)} + \alpha_{01}^{(1)}) \, \xi_{j,0}(\hat{x}_1) + (\alpha_{10}^{(1)} + \alpha_{11}^{(1)}) \, \eta_{j,\nu_{j,1}}(\hat{x}_1) \right),$$

we enforce $v^{(1)}_{|\Gamma_1} \equiv 0$ if and only if the relations $\alpha_{00}^{(1)} + \alpha_{01}^{(1)} = 0$ and $\alpha_{10}^{(1)} + \alpha_{11}^{(1)} = 0$ are satisfied. In other words, $v^{(1)}$ has to be written as

$$v^{(1)}(x) = \sqrt{2} \left(\alpha_{01}^{(1)} \xi_{j,0}(\hat{x}_1) + \alpha_{11}^{(1)} \eta_{j,\nu_{j,1}}(\hat{x}_1) \right) \eta^D_{j,\nu_{j,1}}(\hat{x}_2),$$

where $\eta^D_{j,\nu_{j,1}}$ is the univariate wavelet vanishing at 0, defined in (2.9). Since $v^{(1)}$ has already been set to 0 at C, we now enforce the linear combination

$$-(\alpha_{00}^{(1)} + \alpha_{01}^{(1)}) + (\alpha_{10}^{(1)} + \alpha_{11}^{(1)}) = 0.$$

The matrix containing the matching and boundary conditions along the sides takes the form

$$\mathcal{C}_1^{\text{Mix}} = \begin{pmatrix} -\boldsymbol{c}'' & & & & & \\ \boldsymbol{c}' & -\boldsymbol{c}'' & & & & \\ & \ddots & \ddots & & & \\ & & & \boldsymbol{c}' & -\boldsymbol{c}'' & \\ & & & & \boldsymbol{c}' & -\boldsymbol{c}'' \end{pmatrix} \in \mathbb{R}^{N_C \times 4N_C}.$$

Since there is no scaling function associated to C, we end up with the system

$$\mathcal{D}^{\text{Mix}} \boldsymbol{\alpha} = \boldsymbol{0}, \quad \text{with} \quad \mathcal{D}^{\text{Mix}} = \begin{bmatrix} \mathcal{C}_0^{\text{Mix}} \\ \mathcal{C}_1^{\text{Mix}} \end{bmatrix} \in \mathbb{R}^{2N_C \times 4N_C}.$$

Again, $\mathcal{D}^{\text{Mix}}$ is easily shown to have full rank, so that $\dim W_j^C(\Omega) = 2N_C$; this is precisely the number of grid points surrounding C, to which the wavelets are associated (see Figure 5.3, center).

Pure Dirichlet case. In case d), the matching and boundary conditions at C obviously coincide with those of cases b) and c). As far as the conditions at the sides are concerned, working out as before we end up with the matrix

$$\mathcal{C}_1^{\text{Dir}} = \begin{pmatrix} -\boldsymbol{c}'' & & & & \\ \boldsymbol{c}' & -\boldsymbol{c}'' & & & \\ & & \ddots & \ddots & \\ & & & \boldsymbol{c}' & -\boldsymbol{c}'' \\ & & & & \boldsymbol{c}' \end{pmatrix} \in \mathbb{R}^{(N_C+1) \times 4N_C}$$

and the whole system takes the form

$$\boldsymbol{\mathcal{D}}^{\mathrm{Dir}}\,\boldsymbol{\alpha}=\mathbf{0},\qquad \text{with}\quad \boldsymbol{\mathcal{D}}^{\mathrm{Dir}}=\begin{bmatrix}\boldsymbol{C}_0^{\mathrm{Mix}}\\ \boldsymbol{C}_1^{\mathrm{Dir}}\end{bmatrix}\in I\!\!R^{(2N_C+1)\times 4N_C}.$$

Once again, $\boldsymbol{\mathcal{D}}^{\mathrm{Dir}}$ has full rank, so that $\dim W_j^C(\Omega)=2N_C-1$ (see Figure 5.3, right).

5.2.1. Wavelets with minimal support. Let us first remark that, as for the interior cross point case, a wavelet supported in only one subdomain Ω_i, $i=2,\ldots,N_C-1$ has to satisfy (5.7). In the pure Neumann case, the extra orthogonality condition to $\tilde{\varphi}_{j,C}$ makes the existence of such a wavelet impossible. Conversely, in the mixed Dirichlet/Neumann- and pure Dirichlet cases, its existence is indeed possible.

Pure Neumann case. Let us try to construct wavelets that are supported only in Ω_1, Ω_{N_C}, respectively. The corresponding conditions read

$$\boldsymbol{c}_0\cdot\boldsymbol{\alpha}^{(1)}=\boldsymbol{c}'\cdot\boldsymbol{\alpha}^{(1)}=0,\qquad \boldsymbol{c}_0\cdot\boldsymbol{\alpha}^{(N_C)}=\boldsymbol{c}''\cdot\boldsymbol{\alpha}^{(N_C)}=0, \tag{5.12}$$

which leads to $\boldsymbol{\alpha}^{(1)}=(a,b,-a,-b)$ and $\boldsymbol{\alpha}^{(N_C)}=(a,-a,b,-b)$. Adding the orthogonality condition yields, as before, $a=0$. Choosing $b=1$, we are led to define the following functions:

$$\psi_{j,C}^{0}(x):=\begin{cases}\hat{\psi}_{01}(\hat{x})-\hat{\psi}_{11}(\hat{x}), & x\in\Omega_1,\\ 0, & \text{elsewhere},\end{cases}$$

$$\psi_{j,C}^{2N_C-1}(x):=\begin{cases}\hat{\psi}_{10}(\hat{x})-\hat{\psi}_{11}(\hat{x}), & x\in\Omega_{N_C},\\ 0, & \text{elsewhere};\end{cases}$$

in addition, let us define $\psi_{j,C}^{l}$ for $l=2i-1$, $i\in\{1,\ldots,N_C-1\}$ as in (5.9), $\psi_{j,C}^{l}$ for $l=2i$, $i\in\{1,\ldots,N_C-1\}$ as in (5.10) and $\psi_{j,C}^{2N_C}\equiv\psi_{j,C}^{\mathrm{glob}}$ as in (5.11). These are $2N_C+1$ functions (the same number as the dimension of $W_j^C(\Omega)$); two of them are supported in exactly one subdomain, one is supported in all the subdomains matching at C, while the remaining ones are supported across two consecutive subdomains.

Let us now show that these functions are linearly independent. Indeed, let $\psi:=\sum_{m=0}^{2N_C}\lambda_m\psi_{j,C}^m$ be such that $\psi\equiv 0$. Now, $\psi(C)=0$ implies $\lambda_{2N_C}=0$. On the other hand, $\psi_{|\Gamma_1}\equiv 0$ implies $\lambda_1=0$, and $\psi_{|\Gamma_{N_C}}\equiv 0$ implies $\lambda_{2N_C-1}=0$. Thus, we are left with the same situation as in the interior cross point case.

Pure Dirichlet case. As mentioned above, since in this case we do not have to enforce the orthogonality condition to $\tilde{\varphi}_{j,C}$, one can construct wavelets that are supported in only one subdomain. These are defined as follows

$$\psi_{j,C}^{2i-1}(x):=\begin{cases}\hat{\psi}_{00}(\hat{x})-\hat{\psi}_{01}(\hat{x})-\hat{\psi}_{10}(\hat{x})+\hat{\psi}_{11}(\hat{x}), & x\in\Omega_i,\\ 0, & \text{elsewhere},\end{cases} \tag{5.13}$$

for $i\in\{1,\ldots,N_C\}$; they are precisely the functions introduced in (5.8) with $a=1$. In addition, one has the wavelets $\psi_{j,C}^{2i}$, $i\in\{1,\ldots,N_C-1\}$ defined in (5.10), which are supported in $\bar{\Omega}_i\cup\bar{\Omega}_{i+1}$. No function supported in all the subdomains surrounding C is needed.

We have defined a system of $2N_C-1$ functions, which is precisely the dimension of $W_j^C(\Omega)$. The linear independence of these functions is readily seen. Indeed, since the linear combination $\psi:=\sum_{m=1}^{2N_C-1}\lambda_m\,\psi_{j,C}^m\equiv 0$ must vanish on all sides, we obtain that the coefficients corresponding to the even indices are zero. Next, considering all the subdomains, we get that the coefficients corresponding to the odd indices also vanish.

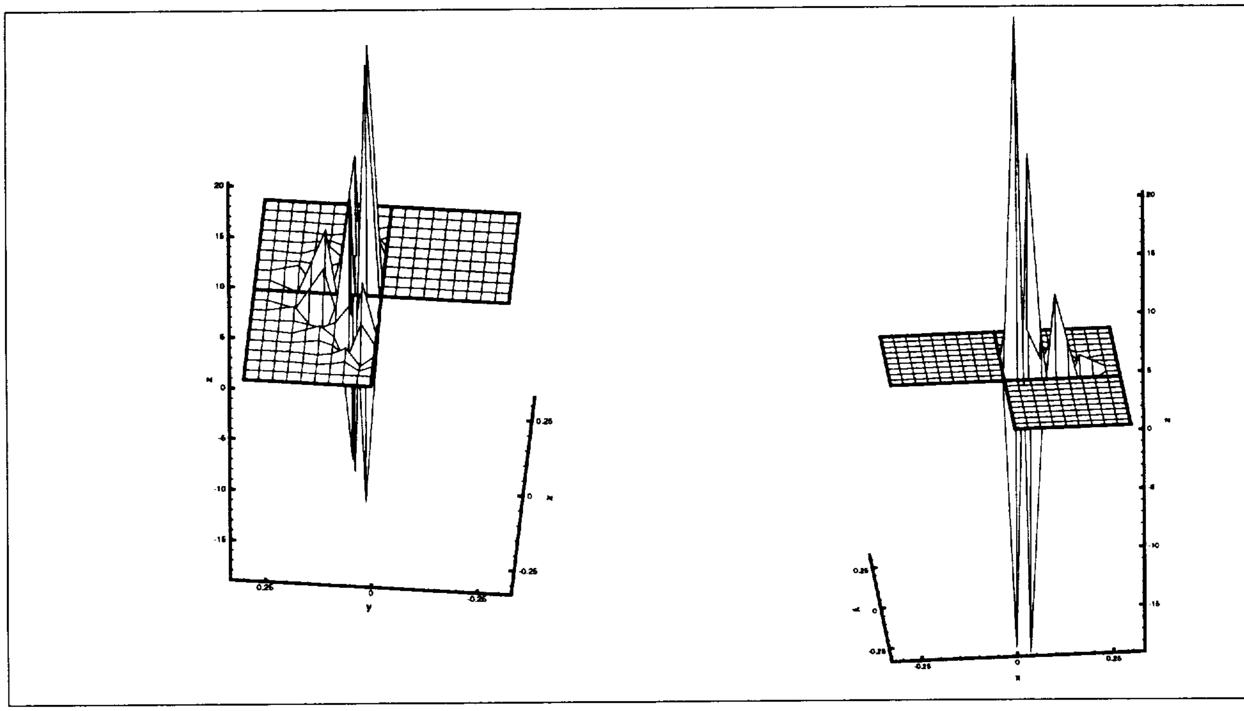

FIG. 5.4. *Wavelets $\psi^2_{j,C}$ and $\psi^3_{j,C}$ around a Dirichlet boundary cross point. (Note again that only a portion of each subdomain around C is shown.)*

Mixed Dirichlet/Neumann case. Again, no orthogonality condition to $\tilde{\varphi}_{j,C}$ is needed. So, we use the system of functions constructed for the pure Dirichlet case, to which we add one function. Precisely, if $\Gamma_1 \subset \Gamma_{\mathrm{Neu}}$, we add the function

$$\psi^0_{j,C}(x) := \begin{cases} \hat{\psi}_{10}(\hat{x}) - \hat{\psi}_{00}(\hat{x}), & x \in \Omega_1, \\ 0, & \text{elsewhere.} \end{cases}$$

If $\Gamma_{N_C} \subset \Gamma_{\mathrm{Neu}}$, we add the function

$$\psi^{2N_C}_{j,C}(x) := \begin{cases} \hat{\psi}_{01}(\hat{x}) - \hat{\psi}_{00}(\hat{x}), & x \in \Omega_{N_C}, \\ 0, & \text{elsewhere.} \end{cases}$$

These functions are continuous and supported in Ω_1, Ω_{N_C}, resp. (note that they correspond to the solutions $\boldsymbol{\alpha}^{(1)} = (-1, 0, 1, 0)$, $\boldsymbol{\alpha}^{(N_C)} = (-1, 1, 0, 0)$, resp., of (5.12)). As a whole, we have $2N_C$ functions, so the dimension of $W^C_j(\Omega)$ is matched. Finally, the linear independence is obvious. Indeed, assuming for instance $\Gamma_1 \subset \Gamma_{\mathrm{Neu}}$, the linear combination $\psi := \sum_{m=0}^{2N_C-1} \lambda_m \psi^m_{j,C} \equiv 0$ must vanish on Γ_1; this implies $\lambda_0 = 0$ and reduces the problem to the pure Dirichlet case.

Example (continued). *We consider an L-shaped domain made up by 3 square subdomains meeting at C. We enforce homogeneous Dirichlet conditions on the whole boundary. The two different types of wavelets produced by our construction are displayed in Figure 5.4.* □

5.3. Matched wavelets across a side. Let us consider two subdomains Ω_+ and Ω_- having a common side $\sigma := \bar{\Omega}_+ \cap \bar{\Omega}_-$. Moreover, let us denote by A and B the two endpoints of σ. As in the cross point case, we may reduce ourselves to a reference situation. Instead of thinking each subdomain as the image of the reference domain $\hat{\Omega}$, here it is natural to think Ω_- (Ω_+, resp.) as the image of the domain $I_- \times I_+$ ($I_+ \times I_+$, resp.), with

$$A = F_-(0,0) = F_+(0,0), \qquad B = F_-(0,1) = F_+(0,1). \tag{5.14}$$

Since the reasoning for the reduction to the reference situation is analogous to the cross point case, we drop these arguments here. Now, (5.14) implies that the set of grid points on σ is given by

$$\begin{aligned}\mathcal{H}_\sigma &:= \{h \,:\, h = F_+(0,\hat{h}_2),\ \hat{h}_2 \in \Delta_j \cup \nabla_j\} \\ &= \{h \,:\, h = F_-(0,\hat{h}_2),\ \hat{h}_2 \in \Delta_j \cup \nabla_j\}.\end{aligned}$$

The grid points $F_+(0,\nu_{j,1})$ and $F_+(0,\nu_{j,M_j})$ are already associated to wavelets $\psi_{j,h}$, since these points correspond to the cross points A and B, respectively. Hence, we are left with the points

$$\mathcal{H}_\sigma^{int} := \mathcal{H}_\sigma \setminus \{F_+(0,\nu_{j,1}), F_+(0,\nu_{j,M_j})\}.$$

Let us first consider the case $h \in \mathcal{H}_\sigma^{int}$ with $\hat{h}_2 \in \Delta_j$. Consequently, there exists a scaling function

$$\varphi_{j,h}(x) := \frac{1}{\sqrt{2}}\xi_{j,\hat{h}_2}(\hat{x}_2)\begin{cases}\xi_{j,1}(\hat{x}_- + 1), & \text{if } x = F_-(\hat{x}_-,\hat{x}_2) \in \Omega_-,\\ \xi_{j,0}(\hat{x}_+), & \text{if } x = F_+(\hat{x}_+,\hat{x}_2) \in \Omega_+,\\ 0, & \text{elsewhere,}\end{cases}$$

associated to h. The basis functions of the local spaces $V_{j+1}^h(\Omega_\pm)$ are then given by

$$\psi_e^-(x) := \xi_{j,\hat{h}_2}(\hat{x}_2)\begin{cases}\xi_{j,1}(\hat{x}_- + 1), & e = 0,\\ \eta_{j,\nu_{j,M_j}}(\hat{x}_- + 1), & e = 1,\end{cases} \qquad \psi_e^+(x) := \xi_{j,\hat{h}_2}(\hat{x}_2)\begin{cases}\xi_{j,0}(\hat{x}_+), & e = 0,\\ \eta_{j,\nu_{j,1}}(\hat{x}_+), & e = 1.\end{cases}$$

This shows that the matching at h is equivalent to the matching at a univariate interface point. Considering the wavelet functions $\hat{\psi}_j^l$ defined in (4.7) for $l = -,+$, we end up with the two wavelets

$$\psi_{j,h_\pm}(x) = \begin{cases}(\hat{\psi}_j^\pm \otimes \xi_{j,\hat{h}_2})(\hat{x}), & x \in \overline{\Omega_- \cup \Omega_+},\\ 0, & \text{elsewhere,}\end{cases}$$

which will be associated to the grid points $h_- := F_-(\nu_{j,M_j},\hat{h}_2)$ and $h_+ := F_+(\nu_{j,1},\hat{h}_2)$, respectively.

Finally, we have to enforce the matching conditions along points $h \in \mathcal{H}_\sigma^{int}$, where $\hat{h}_2 \in \nabla_j$. In this case there is no scaling function associated to h. Again we are reduced to the univariate interface point case, but now in the situation considered in Subsection 4.2. Considering the basis functions $\hat{\vartheta}_j^l$ defined in (4.9) for $l = -,0,+$, we end up with three wavelets

$$\psi_{j,h_l}(x) = \begin{cases}(\hat{\vartheta}_j^l \otimes \eta_{j,\hat{h}_2})(\hat{x}), & x \in \overline{\Omega_- \cup \Omega_+},\\ 0, & \text{elsewhere,}\end{cases}$$

which will be associated to the grid points $h_- := F_-(\nu_{j,M_j},\hat{h}_2)$, $h_0 =: F_-(1,\hat{h}_2) = F_+(0,\hat{h}_2)$ and $h_+ := F_+(\nu_{j,1},\hat{h}_2)$.

6. Trivariate matched wavelets. In this section, the exposition will be deliberately less detailed than in the two previous sections, as the three dimensional construction follows the same spirit presented before. We shall be mainly concerned with the matching around a cross point. The matching around an edge or across a face will be easily reduced to lower dimensional situations.

6.1. Matched wavelets around a cross point. Let us first assume that the cross point C belongs to Ω. Let $N_C = N_{C,3}$ denote the number of subdomains meeting at C, and let these subdomains be (re-)labeled by $\Omega_1, \ldots, \Omega_{N_C}$. It is not restrictive to assume that for all $i \in \{1, \ldots, N_C\}$, one has $C = F_i(0,0,0)$.

It will be useful to express the number $N_{C,2}$ of faces and the number $N_{C,1}$ of edges meeting at C as a function of N_C. This can be accomplished as follows. Consider the tetrahedron in $\bar{\hat{\Omega}}$

$$\hat{T} := \{(\hat{x}_1, \hat{x}_2, \hat{x}_3) \ : \ \hat{x}_1 \geq 0,\ \hat{x}_2 \geq 0,\ \hat{x}_3 \geq 0,\ \hat{x}_1 + \hat{x}_2 + \hat{x}_3 \leq 1\}$$

and, for each $i \in \{1, \ldots, N_C\}$, set $T_i := F_i(\hat{T})$. Then, $P_C := \bigcup_i T_i$ is a (distorted) polyhedron in $I\!R^3$, with the following property: each face (or edge or vertex, resp.) of P_C is in one-to-one correspondence with a subdomain (or face or edge, resp.) meeting at C. Thus, by Euler's polyhedron Theorem, we get

$$N_{C,3} - N_{C,2} + N_{C,1} = 2.$$

On the other hand, since each face of P_C is a (distorted) triangle and each edge of P_C is shared by exactly two faces, one has $3N_{C,3} = 2N_{C,2}$. It follows that

$$N_{C,2} = \tfrac{3}{2} N_C, \qquad N_{C,1} = \tfrac{1}{2} N_C + 2. \tag{6.1}$$

The grid points $h \in \mathcal{H}_j$, to which we are going to associate the matched wavelets, have the form

$$h_{C,i,e} = F_i(\zeta_{e_1}, \zeta_{e_2}, \zeta_{e_3}), \qquad i \in \{1, \ldots, N_C\}, \quad e \in E^3 \setminus \{(0,0,0)\}, \tag{6.2}$$

with

$$\zeta_{e_l} := \begin{cases} 0, & \text{if } e_l = 0, \\ \nu_{j,1}, & \text{if } e_l = 1. \end{cases}$$

Note that there is exactly one of such points which lies inside each subdomain, each face and each edge meeting at C. Thus, the total number of such points is

$$N_{C,3} + N_{C,2} + N_{C,1} = 3N_C + 2.$$

This is precisely the number of wavelets to be constructed around C. Indeed, define for each $e \in E^3$

$$\psi_e^{(i)}(x) = \hat{\psi}_e(\hat{x}) = \theta_{e_1}(\hat{x}_1)\theta_{e_2}(\hat{x}_2)\theta_{e_3}(\hat{x}_3),$$

where

$$\theta_{e_l} := \begin{cases} \xi_{j,0}, & \text{if } e_l = 0, \\ \eta_{j,\nu_{j,1}}, & \text{if } e_l = 1. \end{cases}$$

Let us consider the spaces

$$V_{j+1}^C(\Omega_i) := \text{span}\{\psi_e^{(i)} : e \in E^3\} = \{v^{(i)} = \sum_{e \in E^3} \alpha_e^{(i)} \psi_e^{(i)} \ : \ \boldsymbol{\alpha}^{(i)} := (\alpha_e^{(i)})_{e \in E^3} \in I\!R^3\}$$

and let us introduce the column vector $\boldsymbol{\alpha} := (\boldsymbol{\alpha}^{(i)})_{i=1,\ldots,N_C} \in I\!R^{8N_c}$ (8 being the cardinality of E^3). In order to characterize the local space

$$V_{j+1}^C(\Omega) := \{v \in C^0(\bar{\Omega}) \ : \ v_{|\Omega_i} \in V_{j+1}^C(\Omega_i) \text{ if } i \in \{1, \ldots, N_C\},\ v_{|\Omega_i} \equiv 0 \text{ elsewhere}\},$$

we enforce continuity firstly at C, secondly at the edges and finally at the faces meeting at C. This gives $N_C - 1$ conditions at C, which can be written as

$$\mathcal{C}_0 \boldsymbol{\alpha} = \mathbf{0}, \qquad \text{where} \qquad \mathcal{C}_0 = \begin{pmatrix} c_0 & -c_0 & & \\ & \ddots & \ddots & \\ & & c_0 & -c_0 \end{pmatrix} \in \mathbb{R}^{(N_C-1)\times 8N_C},$$

with $c_0 = (1,1,1,1,1,1,1,1)$. Next, we have $N_{ed} - 1$ conditions at each edge, where N_{ed} is the number of subdomains meeting at the edge; all these conditions can be written as $\mathcal{C}_1 \boldsymbol{\alpha} = \mathbf{0}$, for a suitable matrix $\mathcal{C}_1$ whose structure depends on the topology of the subdomains. Finally, we have 1 condition at each face; they can be represented as $\mathcal{C}_2 \boldsymbol{\alpha} = \mathbf{0}$.

In addition, we want to build functions in $W_j^C(\Omega) := \{v \in V_{j+1}^C(\Omega) : \langle v, \tilde{\varphi}_{j,C}\rangle_\Omega = 0\}$; this adds the condition $\mathcal{B}\boldsymbol{\alpha} = \mathbf{0}$, with $\mathcal{B} := (\boldsymbol{b}, \dots, \boldsymbol{b})$ and $\boldsymbol{b} = (1,0,0,0,0,0,0,0)$. Summarizing, we have

$$\mathcal{D}\,\boldsymbol{\alpha} = \mathbf{0} \qquad \text{with} \qquad \mathcal{D} = \begin{bmatrix} \mathcal{C}_0 \\ \mathcal{C}_1 \\ \mathcal{C}_2 \\ \mathcal{B} \end{bmatrix}.$$

All the conditions that we have enforced are linearly independent, as shown in [4] (see Section 5.2); thus, their number is

$$(N_C - 1) + \sum_{edges} (N_{ed} - 1) + N_{C,2} + 1 = N_C + 3N_C - N_{C,1} + N_{C,2} = 5N_C - 2.$$

Indeed, since each subdomain contains 3 edges meeting in C, one has

$$\sum_{edges} (N_{ed} - 1) = 3N_C - N_{C,1}.$$

We conclude that $\dim W_j^C(\Omega) = 3N_C + 2$, as desired. After the dual construction is made, biorthogonalization is accomplished as described in the previous sections; we omit the details. In conclusion, we end up with $3N_C + 2$ primal and dual wavelets $\psi_{j,C}^l$ and $\tilde{\psi}_{j,C}^l$, $l = 1, \dots, 3N_C + 2$; they are associated to the grid points (6.2), which from now on will be indicated by $h_{C,l}$.

Wavelets with localized support. Let us first notice that, as in lower dimension, no function in $W_j^C(\Omega)$ exists, which is supported in only one subdomain Ω_i. On the contrary, it is easily seen that for each couple of continguous subdomains, two linearly independent functions in $W_j^C(\Omega)$ can be built, which vanish identically outside the two subdomains.

Thus, to each point $h_{C,l}$ which lies inside the common face of two subdomains, we associate one of such wavelet. To all but one points $h_{C,l}$ lying inside the subdomains, we associate other such wavelets, choosing them to be linearly independent from the previous ones. To each point $h_{C,l}$ lying inside an edge, we associate a wavelet supported in the closure of the union of all subdomains sharing the edge: it has the local structure of a tensor product of a two-dimensional scaling function $\varphi_{j,C}$ times the wavelet η_{j,ν_1} in the direction of the edge. Finally, to the remaining point $h_{C,l}$ interior to a subdomain, we associate the global wavelet, which is the three-dimensional analog of (5.11).

Tensor products of matched functions. According to (6.1), the number of subdomains meeting at C is even. We consider here the particular situation in which these subdomains can be grouped in two sets of equal cardinality $N_C/2$, all the subdomains of each set sharing a common edge stemming from C. For instance, this is the relevant case of 8 subdomains meeting at C, and representing the images of unit cubes lying in the 8 octants of $I\!R^3$.

By possibly introducing additional parametric mappings, we may reduce ourselves to the situation in which $N_C/2$ subdomains lie in the upper half space $\hat{x}_3 > 0$ while the remaining ones lie in the lower half plane. Each upper subdomain Ω_i can be written as $\Omega_i = \Omega_i' \times (0,1)$, where Ω_i' is a 2D subdomain in the plane $\hat{x}_3 = 0$; the companion lower subdomain is $\Omega_i' \times (-1,0)$. Thus, we are led to consider the case of $N_C/2$ subdomains in the plane meeting at $C' = (0,0)$. Let φ_j^{II} be the bivariate scaling function associated to C', and let $\psi_j^{II,l}$ $(l = 1,\ldots,N_C/2)$ be any system of bivariate wavelets around C, built as in Subsection 5.1. Moreover, let $\hat{\psi}_j^{I,l}$ $(l = -,+)$ be the univariate wavelets defined in Subsection 4.1, and let $\hat{\vartheta}_j^{I,l}$ $(l = -,0,+)$ the univariate matched functions defined in Subsection 4.2. Then, a system of wavelets around C can be defined as follows:

The functions $\psi_j^{II,l} \otimes \hat{\vartheta}_j^{I,+}$, with $l = 1,\ldots,N_C/2$, are associated to the grid points having a strictly positive $\hat{x}_3$–component and not lying on the $\hat{x}_3$–axis; the functions $\psi_j^{II,l} \otimes \hat{\vartheta}_j^{I,0}$ and $\psi_j^{II,l} \otimes \hat{\vartheta}_j^{I,-}$ are associated to the analogous grid points having zero or negative $\hat{x}_3$–component. Finally, the functions $\varphi_j^{II} \otimes \hat{\psi}_j^{I,\pm}$ are associated to the remaining grid points on the $\hat{x}_3$–axis (obviously, these functions are extended by zero outside the union of the subdomains).

In the case of 8 subdomains meeting at C, the bivariate scaling and wavelet functions may be chosen to be themselves tensor products of univariate matched functions, so one can obtain a fully tensorized local wavelet basis around C.

Cross points lying on the boundary. Let us now assume that the cross point C belongs to $\partial\Omega$. We follow the same notation as before. The grid points $h \in \mathcal{H}_j$ around C to which wavelets will be associated are again of the form (6.2), but now the points lying on a face or an edge contained in $\bar{\Gamma}_{\mathrm{Dir}}$ are missing. Let us denote by $N_{C,2}^{\mathrm{Dir}}$ ($N_{C,1}^{\mathrm{Dir}}$, resp.) the number of faces (edges, resp.) containing C and contained in $\bar{\Gamma}_{\mathrm{Dir}}$. It is easily seen that the number l_C of grid points $h_{C,l}$ we are interested in is

$$l_C = N_{C,3} + (N_{C,2} - N_{C,2}^{\mathrm{Dir}}) + (N_{C,1} - N_{C,1}^{\mathrm{Dir}}).$$

Let us count the number of conditions that define the space $W_j^C(\Omega)$. We have $N_{C,3} - 1$ matching conditions at C, plus one vanishing condition if $C \in \bar{\Gamma}_{\mathrm{Dir}}$ or one orthogonality condition if $C \notin \bar{\Gamma}_{\mathrm{Dir}}$. Next, we have $N_{ed} - 1$ matching conditions at each edge, plus one vanishing condition at each edge contained in $C \in \bar{\Gamma}_{\mathrm{Dir}}$. Finally, let N_f indicate the number of subdomains sharing the face f (this is 2 if the face is not contained in $\partial\Omega$, 1 if it is); then, we have $N_f - 1$ matching conditions at each face, plus one vanishing condition at each face contained in $C \in \bar{\Gamma}_{\mathrm{Dir}}$. Observing that

$$\sum_{edges} N_{ed} = \sum_{faces} N_f = 3N_{C,3},$$

the total number t_C of conditions which define $W_j^C(\Omega)$ is

$$t_C = 7N_{C,3} - (N_{C,2} - N_{C,2}^{\mathrm{Dir}}) - (N_{C,1} - N_{C,1}^{\mathrm{Dir}}).$$

Since these conditions are linearly independent (see again [4]), we obtain, as desired,

$$\dim W_j^C(\Omega) = 8N_{C,3} - t_C = l_C.$$

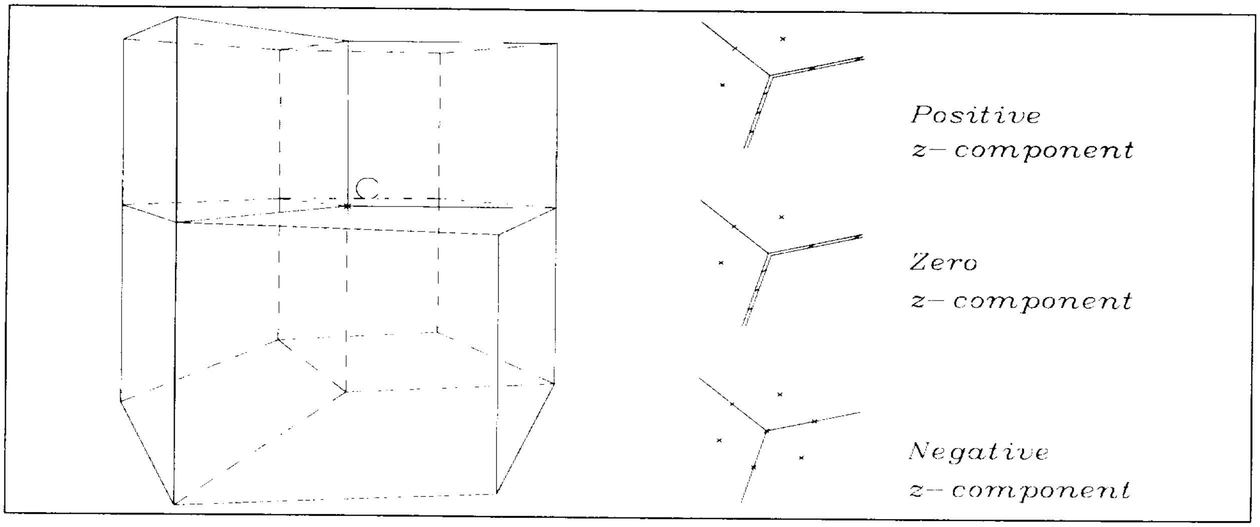

FIG. 6.1. *Example of* 5 *trivariate subdomains meeting at a cross point belonging to the Dirichlet part of the boundary (left). The pictures in the right column show the wavelet grid points having positive, zero and negative* z*–component, respectively (from top to bottom).*

As in the interior cross point case, wavelets can be constructed with localized support. Actually, if $C \in \bar{\Gamma}_{\mathrm{Dir}}$, wavelets exist which are supported within one subdomain; they will be associated to the point $h_{C,l}$ lying inside the corresponding subdomain.

Example. *Let us consider the domain represented in Figure 6.1 which is divided into* 5 *subdomains. Let us assume that the three boundary faces meeting at* C *are contained in* Γ_{Dir}. *We want to exhibit one particular choice of wavelets around* C, *which can easily be constructed. To this end, let us assume that* $C = (0,0,0)$ *and let us divide the wavelet grid points around* C *into three sets, corresponding to their third coordinate* z *being negative, zero or positive as indicated in Figure 6.1.*

For defining the wavelets associated to the grid points having $z < 0$, *consider the bivariate scaling function* φ_j^{II} *and the bivariate wavelets* $\psi_j^{II,l}$ $(l = 1,\ldots,6)$ *associated to a 2D interior cross point* C' *common to three subdomains. In addition, let* $\hat{\vartheta}_j^{I,-}$ *be the matched univariate function defined in* (4.9) *and having support in* $(-1,0)$. *Then, we associate to these grid points the 7 wavelets*

$$\begin{array}{ll} \varphi_j^{II} \otimes \hat{\vartheta}_j^{I,-} & \text{(to the grid point on the } z\text{-axis)} \\ \psi_j^{II,l} \otimes \hat{\vartheta}_j^{I,-},\ (l = 1,\ldots,6) & \text{(to the grid points around the axis).} \end{array}$$

It remains to define wavelets associated to those wavelet grid points having zero or positive third component. To this end, let $\check{\psi}_j^{II,l}$ $(l = 1,\ldots,3)$ *be the system of wavelets associated to a 2D Dirichlet boundary cross point common to two subdomains. Then, the functions* $\check{\psi}_j^{II,l} \otimes \hat{\vartheta}_j^{I,0}$ $(l = 1,2,3)$ *will be associated to the three wavelet grid points with* $z = 0$ *and the analogous three grid points in the upper half space are identified with the wavelets* $\check{\psi}_j^{II,l} \otimes \hat{\vartheta}_j^{I,+}$ $(l = 1,2,3)$.

Note that no extra orthogonality to dual scaling functions has to be enforced, since no scaling function is associated to the 3D Dirichlet cross point C. □

6.2. Matched wavelets around an edge or a face. Let $\sigma = ed$ be an edge, at which N_{ed} subdomains meet. We can reduce ourselves to the situation in which the subdomains are (re-)labeled by $\Omega_1,\ldots,\Omega_{N_{ed}}$ and for each $i \in \{1,\ldots,N_{ed}\}$ we have

$$ed = \{\, F_i(0,0,\zeta) \;:\; 0 \le \zeta \le 1 \,\}.$$

It is enough to consider points $h_{ed} \in \mathcal{K}_{j+1}$ which are internal to ed. Precisely, if $h_{ed} = F_i(0,0,\hat{h}_3)$ with $\hat{h}_3 \in \Delta_j^{int}$, then we build wavelets which, in local coordinates, can be written as $\hat{\psi}^l_{j,ed} \otimes \xi_{j,\hat{h}_3}$, where $\hat{\psi}^l_{j,ed}$ are matched bivariate wavelets as defined in subsections 5.1 or 5.2. They will be associated to the points $h \in \mathcal{H}_j$ having the form $h = F_i(\zeta_1, \zeta_2, \hat{h}_3)$, with $\zeta_1, \zeta_2 \in \{0, \nu_{j,1}\}$.

On the other hand, if $h_{ed} = F_i(0,0,\hat{h}_3)$ with $\hat{h}_3 \in \nabla_j^{int}$, then the wavelets will be locally represented as $\psi^l_{j,ed} \otimes \eta_{j,\hat{h}_3}$, where now $\psi^l_{j,ed}$ are matched bivariate wavelets, defined as in the previously quoted Subsections, but without enforcing the biorthogonality condition $\boldsymbol{B\alpha} = \mathbf{0}$. The association to the grid points surrounding h_{ed} is done as above (note that now $h_{ed} \in \mathcal{H}_j$).

At last, let $\sigma = f$ be a face common to two subdomains Ω_- and Ω_+. The reference situation is such that

$$f = \{\, F_+(0, \zeta_2, \zeta_3) \;:\; 0 \le \zeta_2, \zeta_3 \le 1 \,\}.$$

Let $h_f \in \mathcal{K}_{j+1}$. If $h_f = F_+(0, \hat{h}_2, \hat{h}_3)$ with $\hat{h}_2, \hat{h}_3 \in \Delta_j^{int}$, then we build wavelets having the local representation $\hat{\psi}^l_{j,f} \otimes \xi_{j,\hat{h}_2} \otimes \xi_{j,\hat{h}_3}$, where $\hat{\psi}^l_{j,f}$ are matched univariate wavelets as defined in Subsection 4.1. On the other hand, if $h_f = F_+(0, \hat{h}_2, \hat{h}_3)$ with $\hat{h}_2, \hat{h}_3 \in \Delta_j^{int} \cup \nabla_j^{int}$ and at least one coordinate in ∇_j^{int}, then the local representation of the wavelets will be one of the following ones:

$$\hat{\vartheta}^l_{j,f} \otimes \eta_{j,\hat{h}_2} \otimes \xi_{j,\hat{h}_3}, \quad \hat{\vartheta}^l_{j,f} \otimes \xi_{j,\hat{h}_2} \otimes \eta_{j,\hat{h}_3}, \quad \hat{\vartheta}^l_{j,f} \otimes \eta_{j,\hat{h}_2} \otimes \eta_{j,\hat{h}_3},$$

where now $\hat{\vartheta}^l_{j,f}$ are matched univariate functions built in Subsection 4.2. The association of these wavelets to the grid points surrounding h_f is straightforward.

Appendix A. Mask coefficients. In this appendix we provide all the mask (filter) coefficients of the univariate scaling functions and wavelets for our B–spline example $L = 2$ and $\tilde{L} = 4$. These are the data that are needed to reproduce the figures in this paper and to use these functions, e.g., as trial functions for numerically solving differential and integral equations. Starting from the masks of the univariate functions, those for multivariate and matched functions can easily be obtained by appropriate tensorization, using the matching coefficients given in the paper at any interface among subdomains.

Refinement coefficients. Let us start with the refinement coefficients on the real line corresponding to the equations

$$\phi(x) = 2^{-1/2} \sum_{k \in \mathbb{Z}} a_k\, \phi(2x - k), \qquad \tilde{\phi}(x) = 2^{-1/2} \sum_{k \in \mathbb{Z}} \tilde{a}_k\, \tilde{\phi}(2x - k),$$

where the coefficients here are given by ([8]):

$$a_{-1} = 5.000000000000e-01, \quad a_0 = 1.000000000000e+00, \quad a_1 = 5.000000000000e-01,$$

for the primal scaling function, and by

$$\begin{aligned}
\tilde{a}_{-4} &= 4.687500000000e-02, & \tilde{a}_{-3} &= -9.375000000000e-02, & \tilde{a}_{-2} &= -2.500000000000e-01,\\
\tilde{a}_{-1} &= 5.937500000000e-01, & \tilde{a}_{0} &= 1.406250000000e+00, & \tilde{a}_{1} &= 5.937500000000e-01,\\
\tilde{a}_{2} &= -2.500000000000e-01, & \tilde{a}_{3} &= -9.375000000000e-02, & \tilde{a}_{4} &= 4.687500000000e-02,
\end{aligned}$$

for the dual one.

Next, we give the entries of the refinement matrices M_j and $\tilde{M}_j$ for the whole bases Ξ_j, $\tilde{\Xi}_j$, respectively, as defined in (2.3-a). These matrices have the following structure (taken from [11]):

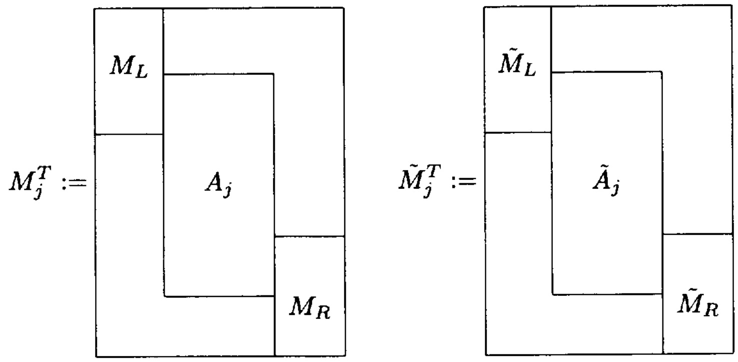

Here, the central blocks A_j and $\tilde{A}_j$ take the form

$$\left(A_j\right)_{m,k} = \frac{1}{\sqrt{2}} a_{m-2k}, \quad 3 \le m \le 2^{j+1} - 3, \quad 2 \le k \le 2^j - 2,$$
$$\left(\tilde{A}_j\right)_{m,k} = \frac{1}{\sqrt{2}} \tilde{a}_{m-2k}, \quad 4 \le m \le 2^{j+1} - 4, \quad 4 \le k \le 2^j - 4,$$

with the previously given coefficients a_k and $\tilde{a}_k$. The upper left blocks are here given by

$$M_L = \begin{bmatrix} 7.071067811865e-01 \\ 4.890821903207e-01 \\ -3.794806392368e-01 \\ -6.010407640086e-02 \\ 1.084230397819e-01 \\ 4.360491817317e-02 \\ -2.121320343560e-02 \\ -1.060660171780e-02 \end{bmatrix}$$

$$\tilde{M}_L = \begin{bmatrix} 7.071067811865e-01 & 0.000000000000e+00 & 0.000000000000e+00 & 0.000000000000e+00 \\ 7.733980419228e-01 & 7.402524115547e-01 & -2.695844603274e-01 & 5.082329989778e-02 \\ -2.209708691208e-01 & 8.175922157469e-01 & -6.187184335382e-02 & 4.419417382416e-03 \\ -3.314563036812e-01 & 4.529902816976e-01 & 3.933281470350e-01 & -5.966213466262e-02 \\ 1.657281518406e-01 & -1.933495104807e-01 & 1.007627163191e+00 & -1.800912583334e-01 \\ 0.000000000000e+00 & -6.629126073623e-02 & 4.198446513295e-01 & 4.198446513295e-01 \\ 0.000000000000e+00 & 3.314563036813e-02 & -1.767766952966e-01 & 9.943689110436e-01 \\ 0.000000000000e+00 & 0.000000000000e+00 & -6.629126073624e-02 & 4.198446513295e-01 \\ 0.000000000000e+00 & 0.000000000000e+00 & 3.314563036812e-02 & -1.767766952966e-01 \\ 0.000000000000e+00 & 0.000000000000e+00 & 0.000000000000e+00 & -6.629126073624e-02 \\ 0.000000000000e+00 & 0.000000000000e+00 & 0.000000000000e+00 & 3.314563036812e-02 \end{bmatrix}.$$

The lower right blocks M_R and $\tilde{M}_R$ arise from their upper left counterparts by reflecting rows and columns in the following way:

$$(M_R)_{2^j-m,2^j-k} = (M_L)_{m,k}, \quad m = 0, \ldots, 8, \ k = 0,$$

and similarly for the dual functions.

Wavelet coefficients. The wavelets on the real line can be written as linear combination of the translates of ϕ on level 1, i.e.,

$$\psi(x) = 2^{-1/2} \sum_{k \in \mathbb{Z}} b_k \, \phi(2x - k), \qquad \tilde{\psi}(x) = 2^{-1/2} \sum_{k \in \mathbb{Z}} \tilde{b}_k \, \tilde{\phi}(2x - k).$$

The corresponding masks for our example are given by

$$
\begin{array}{llllll}
b_1 = & 1.060660171780e-01, & b_2 = & 2.121320343559e-01, & b_3 = & -5.656854249493e-01, \\
b_4 = & -1.343502884254e+00, & b_5 = & 3.181980515339e+00, & b_6 = & -1.343502884254e+00, \\
b_7 = & -5.656854249492e-01, & b_8 = & 2.121320343560e-01, & b_9 = & 1.060660171780e-01,
\end{array}
$$

for the primal wavelets, and by

$$
\tilde{b}_4 = -1.104854345604e-01, \quad \tilde{b}_5 = 2.209708691208e-01, \quad \tilde{b}_6 = -1.104854345604e-01,
$$

for the dual ones ([8]). Let us now consider the two-scale matrices G_j and $\tilde{G}_j$ for the whole wavelet basis, which give the transformation

$$
\Upsilon_j = G_j \Xi_{j+1}, \qquad \tilde{\Upsilon}_j = \tilde{G}_j \tilde{\Xi}_{j+1}.
$$

Again, G_j and $\tilde{G}_j$ have the same block structure as M_j, $\tilde{M}_j$, respectively, possibly with a different size of the blocks. The inner blocks correspond to those of M_j, $\tilde{M}_j$, by replacing a_k, $\tilde{a}_k$ by b_k, $\tilde{b}_k$, respectively. Here, the upper left block of the refinement matrix for the wavelets read:

$$
G_L = \begin{bmatrix}
7.071067811866e-01 & 0.000000000000e+00 \\
-4.890821903207e-01 & 1.237436867076e+00 \\
3.794806392368e-01 & -4.313351365238e+00 \\
6.010407640085e-02 & 4.985102807365e+00 \\
-1.084230397819e-01 & -1.555634918610e+00 \\
-4.360491817317e-02 & -6.717514421272e-01 \\
2.121320343560e-02 & 2.121320343560e-01 \\
1.060660171780e-02 & 1.060660171780e-01
\end{bmatrix}
$$

$$
\tilde{G}_L = \begin{bmatrix}
7.071067811865e-01 & 0.000000000000e+00 \\
-7.733980419228e-01 & -1.473139127472e-02 \\
2.209708691208e-01 & -5.892556509888e-02 \\
3.314563036812e-01 & 1.325825214725e-01 \\
-1.657281518406e-01 & -6.629126073624e-02
\end{bmatrix}.
$$

The lower blocks again arise by reflecting the upper blocks.

Homogeneous boundary conditions. Let us now consider scaling functions and wavelets having homogeneous boundary conditions. For the scaling functions, one only has to eliminate the first and last row in M_j and $\tilde{M}_j$, respectively.

For the corresponding wavelets, we have to modify the first and last wavelet as defined in (2.9). This means changing the first and last column of G_L and $\tilde{G}_L$, respectively, by using the following coefficients instead:

$$
\begin{array}{llllll}
b_0 = & 0.000000000000e+00, & b_1 = & -6.916666666667e-01, & b_2 = & 5.366666666667e-01, \\
b_3 = & 8.500000000000e-02, & b_4 = & -1.533333333333e-01, & b_5 = & -6.166666666667e-02, \\
b_6 = & 3.000000000000e-02, & b_7 = & 1.500000000000e-02, & &
\end{array}
$$

for the primal wavelets, and

$$
\begin{array}{llllll}
\tilde{b}_0 = & 0.000000000000e+00, & \tilde{b}_1 = & -1.093750000000e+00, & \tilde{b}_2 = & 3.125000000000e-01, \\
\tilde{b}_3 = & 4.687500000000e-01, & \tilde{b}_4 = & -2.343750000000e-01, & &
\end{array}
$$

for the dual ones.

The coefficients in the refinement matrices for a whole variety of choices of the parameters L and $\tilde{L}$ (for the construction in [11] based on [8]) can be obtained in MATLAB-format from the homepage of the third author `http://www.igpm.rwth-aachen.de/~urban` under the topic `Software`. The software described in [3] (written in C++) that has been used to produce the pictures in this paper can also be obtained via this website.

Acknowledgement. The authors feel very grateful to Titus Barsch for his assistance in programming and producing the pictures.

REFERENCES

[1] R.A. ADAMS, Sobolev Spaces, Academic Press, 1978.

[2] L. ANDERSSON, N, HALL, B. JAWERTH, AND G. PETERS, *Wavelets on closed subsets of the real line*, in: Topics in the Theory and Applications of Wavelets, L.L. Schumaker and G. Webb, eds., Academic Press, Boston, 1994, pp. 1–61.

[3] T. BARSCH AND K. URBAN *Software tools for using wavelets on the interval for the numerical solution of operator equations*, RWTH Aachen, IGPM, in preparation.

[4] C. CANUTO, A. TABACCO, AND K. URBAN, *The Wavelet Element Method, Part I: Construction and analysis*, Istituto di Analisi Numerica del CNR, Pavia, Preprint No. 1038, 1997. Appl. Comp. Harm. Anal., to appear.

[5] C. CANUTO, A. TABACCO, AND K. URBAN, *Approximation of elliptic problems by the Wavelet Element Method*, in *Proceedings of the 2nd ENUMATH conference*, R. Rannacher ed., Word Scientific co., Singapore, to appear.

[6] G. CHIAVASSA AND J. LIANDRAT, *On the effective construction of compactly supported wavelets satisfying homogeneous boundary conditions on the interval*, Appl. Comp. Harm. Anal., to appear.

[7] A. COHEN, W. DAHMEN, AND R.A. DEVORE, *Multiscale decompositions on bounded domains*, RWTH Aachen, Preprint IGPM No. 113, 1995; Trans. Amer. Math. Soc., to appear.

[8] A. COHEN, I. DAUBECHIES, AND J.-C. FEAUVEAU, *Biorthogonal bases of compactly supported wavelets*, Comm. Pure Appl. Math., **45** (1992), pp. 485–560.

[9] A. COHEN, I. DAUBECHIES, AND P. VIAL, *Wavelets on the interval and fast wavelet transforms*, Appl. Comp. Harm. Anal., **1** (1993), pp. 54–81.

[10] A. COHEN AND R. MASSON *Wavelet adaptive method for second order elliptic problems, boundary conditions and domain decomposition*, in *Proceedings of the 2nd ENUMATH conference*, R. Rannacher ed., Word Scientific co., Singapore, to appear.

[11] W. DAHMEN, A. KUNOTH, AND K. URBAN, *Biorthogonal spline wavelets on the interval — Stability and moment conditions*, RWTH Aachen, Preprint IGPM No. 129, 1996, Appl. Comp. Harm. Anal., to appear.

[12] W. DAHMEN, A. KUNOTH, AND K. URBAN, *Wavelets in Numerical Analysis and their quantitative properties*, in: Surface Fitting and Multiresolution Methods, A. Le Mehaute, C. Rabut, and L.L. Schumaker (eds.), Vanderbilt Univ. Press, Nashville, TN, 1997, pp. 93–130.

[13] W. DAHMEN AND R. SCHNEIDER, *Composite wavelet bases for operator equations*, RWTH Aachen, Preprint IGPM No. 133, 1996.

[14] W. DAHMEN AND R. SCHNEIDER, *Multiscale methods for boundary integral equations I: Biorthogonal wavelets on 2D-manifolds in $\mathbb{R}^3$*, RWTH Aachen, Preprint IGPM No.149, 1998.

[15] A. JOUINI AND P.-G. LEMARIÉ-RIEUSSET, *Analyses multirésolutions biorthogonales et applications*, Ann. Inst. H. Poincaré Anal. Non Linéaire, **10** (1993), pp. 453–476.

[16] C. LAGE AND C. SCHWAB, *Two notes on the implementation of wavelet Galerkin Boundary Element Methods*, ETH Zurich, Tech. Report No. 7, 1997.

[17] L. LEVAGGI AND A. TABACCO, *Wavelets on the interval and related topics*, Dipartimento di Matematica, Politecnico di Torino, Preprint No. 11, 1997.

[18] R. MASSON, *Biorthogonal spline wavelets on the interval for the resolution of boundary problems*, Math. Mod. Meths in Appl. Sci., **6** (1996), 749–791.

REPORT DOCUMENTATION PAGE

Form Approved
OMB No. 0704-0188

1. AGENCY USE ONLY *(Leave blank)*

2. REPORT DATE
April 1998

3. REPORT TYPE AND DATES COVERED
Contractor Report

4. TITLE AND SUBTITLE
The Wavelet Element Method Part II: Realization and Additional Features in 2D and 3D

5. FUNDING NUMBERS
C NAS1-97046
WU 505-90-52-01

6. AUTHOR(S)
Claudio Canuto
Anita Tabacco
Karsten Urban

7. PERFORMING ORGANIZATION NAME(S) AND ADDRESS(ES)
Institute for Computer Applications in Science and Engineering
Mail Stop 403, NASA Langley Research Center
Hampton, VA 23681-2199

8. PERFORMING ORGANIZATION REPORT NUMBER
ICASE Report No. 98-17

9. SPONSORING/MONITORING AGENCY NAME(S) AND ADDRESS(ES)
National Aeronautics and Space Administration
Langley Research Center
Hampton, VA 23681-2199

10. SPONSORING/MONITORING AGENCY REPORT NUMBER
NASA/CR-1998-207637
ICASE Report No. 98-17

11. SUPPLEMENTARY NOTES
Langley Technical Monitor: Dennis M. Bushnell
Final Report
Submitted to Applied and Computational Harmonic Analysis

12a. DISTRIBUTION/AVAILABILITY STATEMENT
Unclassified–Unlimited
Subject Category 64
Distribution: Nonstandard
Availability: NASA-CASI (301)621-0390

12b. DISTRIBUTION CODE

13. ABSTRACT *(Maximum 200 words)*

The Wavelet Element Method (WEM) provides a construction of multiresolution systems and biorthogonal wavelets on fairly general domains. These are split into subdomains that are mapped to a single reference hypercube. Tensor products of scaling functions and wavelets defined on the unit interval are used on the reference domain. By introducing appropriate matching conditions across the interelement boundaries, a globally continuous biorthogonal wavelet basis on the general domain is obtained. This construction does not uniquely define the basis functions but rather leaves some freedom for fulfilling additional features.

In this paper we detail the general construction principle of the WEM to the 1D, 2D and 3D cases. We address additional features such as symmetry, vanishing moments and minimal support of the wavelet functions in each particular dimension. The construction is illustrated by using biorthogonal spline wavelets on the interval.

14. SUBJECT TERMS
wavelets, matched multiscale bases, preconditioning, partial differential equations

15. NUMBER OF PAGES
43

16. PRICE CODE
A03

17. SECURITY CLASSIFICATION OF REPORT	18. SECURITY CLASSIFICATION OF THIS PAGE	19. SECURITY CLASSIFICATION OF ABSTRACT	20. LIMITATION OF ABSTRACT
Unclassified	Unclassified		

NSN 7540-01-280-5500

Standard Form 298(Rev. 2-89)
Prescribed by ANSI Std. Z39-18
298-102